Lidocaine Preferentially Inhibits the Function of Purinergic P2X7 Receptors Expressed in *Xenopus* Oocytes

Dan Okura, MD,* Takafumi Horishita, MD, PhD,* Susumu Ueno, MD, PhD,†
Nobuyuki Yanagihara, PhD,‡ Yuka Sudo, PhD,§ Yasuhito Uezono, MD, PhD,‖ Tomoko Minami, MD,*
Takashi Kawasaki, MD, PhD,* and Takeyoshi Sata, MD, PhD*

BACKGROUND: Lidocaine has been widely used to relieve acute pain and chronic refractory pain effectively by both systemic and local administration. Numerous studies reported that lidocaine affects several pain signaling pathways as well as voltage-gated sodium channels, suggesting the existence of multiple mechanisms underlying pain relief by lidocaine. Some extracellular adenosine triphosphate (ATP) receptor subunits are thought to play a role in chronic pain mechanisms, but there have been few studies on the effects of lidocaine on ATP receptors. We studied the effects of lidocaine on purinergic P2X3, P2X4, and P2X7 receptors to explore the mechanisms underlying pain-relieving effects of lidocaine.
METHODS: We investigated the effects of lidocaine on ATP-induced currents in ATP receptor subunits, P2X3, P2X4, and P2X7 expressed in *Xenopus* oocytes, by using whole-cell, two-electrode, voltage-clamp techniques.
RESULTS: Lidocaine inhibited ATP-induced currents in P2X7, but not in P2X3 or P2X4 subunits, in a concentration-dependent manner. The half maximal inhibitory concentration for lidocaine inhibition was 282 ± 45 μmol/L. By contrast, mepivacaine, ropivacaine, and bupivacaine exerted only limited effects on the P2X7 receptor. Lidocaine inhibited the ATP concentration–response curve for the P2X7 receptor via noncompetitive inhibition. Intracellular and extracellular *N*-(2,6-dimethylphenylcarbamoylmethyl) triethylammonium bromide (QX-314) and benzocaine suppressed ATP-induced currents in the P2X7 receptor in a concentration-dependent manner. In addition, repetitive ATP treatments at 5-minute intervals in the continuous presence of lidocaine revealed that lidocaine inhibition was use-dependent. Finally, the selective P2X7 receptor antagonists Brilliant Blue G and AZ11645373 did not affect the inhibitory actions of lidocaine on the P2X7 receptor.
CONCLUSIONS: Lidocaine selectively inhibited the function of the P2X7 receptor expressed in *Xenopus* oocytes. This effect may be caused by acting on sites in the ion channel pore both extracellularly and intracellularly. These results help to understand the mechanisms underlying the analgesic effects of lidocaine when it is administered locally at least. (Anesth Analg 2015;120:597–605)

Systemic administration of lidocaine has been used to relieve neuropathic pain, including that from malignant and nonmalignant disorders.[1,2] Abnormal expression of voltage-gated sodium channels in both injured and neighboring areas correlates with ectopic activity[3] that has been proposed as a mechanism underlying neuropathic pain,[4] suggesting the role of blockade of specific sodium channels by intravenous lidocaine to produce neuropathic pain relief.[5] However, lidocaine has other several beneficial effects in some clinical situations such as postoperative pain relief by epidural administration, stimulation of bowel function after colon surgery,[6] and topical anesthesia in addition to properties including antithrombotic[7] and anti-inflammatory actions,[8] which are potentially important during the perioperative period. These multiple effects of lidocaine indicate that there may be mechanisms other than sodium channel blockade. Moreover, the difference of effective concentrations between intravenous and epidural administration also supports this possibility. Indeed, several reports demonstrated that lidocaine affects other pain signaling pathways,[9] receptors, and ion channels including Gq protein,[10] potassium channels,[11] and calcium channels.[12]

Extracellular adenosine triphosphate (ATP) is a neurotransmitter acting through ATP receptors, which are classified as ligand-gated ion channels (P2X receptors) and G-protein–coupled receptors (P2Y receptors). Seven P2X (P2X1–7) and eight P2Y (P2Y1, P2Y2, P2Y4, P2Y6, P2Y11–14) subunits have been identified.[13] They are distributed in multiple organs and have important roles in various physiologic functions.[14,15] Recently, specific receptor subunits have been shown to be involved in various pathologic conditions, including brain ischemia, pain, inflammation,

From the *Department of Anesthesiology, School of Medicine, University of Occupational and Environmental Health, Yahatanishiku, Kitakyushu, Fukuoka, Japan; †Department of Occupational Toxicology, Institute of Industrial Ecological Sciences, University of Occupational and Environmental Health, Yahatanishiku, Kitakyushu, Fukuoka, Japan; ‡Department of Pharmacology, School of Medicine, University of Occupational and Environmental Health, Yahatanishiku, Kitakyushu, Fukuoka, Japan; §Department of Molecular Pathology and Metabolic Disease, Faculty of Pharmaceutical Sciences, Tokyo University of Science, Noda, Chiba, Japan; and ‖Cancer Pathophysiology Division, National Cancer Center Research Institute, Chuouku, Tokyo, Japan.

Accepted for publication October 24, 2014.

Funding: This study was supported by a Grant-in-Aid for Scientific Research from Japan Society for the Promotion of Science, 22591756 (to TS).

The authors declare no conflicts of interest.

Address correspondence to Takafumi Horishita, MD, PhD, Department of Anesthesiology, School of Medicine, University of Occupational and Environmental Health, 1-1 Iseigaoka, Yahatanishiku, Kitakyushu, Fukuoka 807–8555, Japan. Address e-mail to thori@med.uoeh-u.ac.jp.

DOI: 10.1213/ANE.0000000000000585

osteoporosis, spinal cord injury, and bladder dysfunction; therefore, these receptors are considered to be potential therapeutic targets.[16–19] It is especially suggested that several subunits including P2X3, P2X4, and P2X7 receptors, which are distributed in pain pathways within the nervous system, are involved in chronic pain mechanisms.[20]

P2X3 receptors, which are mainly distributed in sensory neurons such as dorsal root ganglia, have been shown to be involved in the mechanism of neuropathic pain by demonstrating that intrathecal treatment with P2X3 antisense oligonucleotide decreased nociceptive behavior in a model of chronic inflammation and reduced mechanical allodynia in a rat model of neuropathic pain.[21] P2X4 receptors are widely expressed in the brain, spinal cord, autonomic and sensory ganglia, and microglia. Several reports demonstrated that upregulation of P2X4 receptors in activated microglia located in the dorsal horn of the spinal cord contributes to neuropathic pain.[22] P2X7 receptors are expressed on cells of the immune system as well as glial cells. In addition, inflammatory and neuropathic hypersensitivities in response to mechanical and thermal stimuli were completely absent in mice lacking P2X7 receptors,[23] suggesting a role of P2X7 receptors in pain modulation.

Although previous reports have demonstrated the effects of some general anesthetics, ethanol, and antidepressants on P2X receptors,[24–28] no studies have investigated whether local anesthetics act on these receptors. Therefore, we investigated the effects of lidocaine and other local anesthetics on P2X3, P2X4, and P2X7 receptors to explore the mechanisms underlying the pain-relieving effects of lidocaine.

METHODS

This study was approved by the Animal Research Committee of the University of Occupational and Environmental Health, Kitakyushu, Japan.

Drugs

All chemicals, including ATP disodium salt, lidocaine hydrochloride, ropivacaine hydrochloride, bupivacaine hydrochloride, benzocaine, *N*-(2,6-dimethylphenylcarbamoylmethyl) triethylammonium bromide (QX-314), AZ11645373, and Brilliant Blue G (BBG), were purchased from Sigma-Aldrich (St. Louis, MO).

Plasmids

All plasmids including human P2X3, P2X4, and P2X7 receptor complementary DNA (cDNA) were purchased from OriGene Technologies (Rockville, MD).

cRNA Preparation and Oocyte Injection

After double digestion of cDNA with *Sac*I and *Sma*I (P2X3 receptor) or linearization with *Sac*I (P2X4 and P2X7 receptors), complementary RNAs (cRNA) were transcribed using T7 RNA polymerase using an mMESSAGE mMACHINE kit (Ambion, Austin, TX). Adult female *Xenopus laevis* frogs were obtained from Kyudo (Saga, Japan). *X. laevis* oocytes and cRNA microinjection were prepared and performed as described previously.[29,30] In brief, stage IV to VI oocytes were manually isolated from a removed portion of ovary. Next, oocytes were treated with collagenase (0.5 mg/mL) for 10 minutes and placed in modified Barth solution (88 mmol/L NaCl, 1 mmol/L KCl, 2.4 mmol/L $NaHCO_3$, 10 mmol/L HEPES, 0.82 mmol/L $MgSO_4$, 0.33 mmol/L $Ca[NO_3]_2$, and 0.91 mmol/L $CaCl_2$, adjusted to pH 7.5), supplemented with 10,000 U penicillin, 50 mg gentamicin, 90 mg theophylline, and 220 mg/L sodium pyruvate (incubation medium). cRNAs of P2X receptors were injected (total volume was 0.5–20 ng/50 nL) into *Xenopus* oocytes. Injected oocytes were incubated at 19°C in incubation medium, and 2 to 6 days after injection, the cells were used for electrophysiologic recordings.

Electrophysiologic Recordings

All electrical recordings were performed at room temperature (20–23°C). Oocytes were placed in a 100-μL recording chamber and perfused at 2 mL/min with extracellular Ringer's solution (110 mmol/L NaCl, 2.5 mmol/L KCl, 10 mmol/L HEPES, 1.8 mmol/L $BaCl_2$, pH 7.5) using a peristaltic pump (World Precision Instruments, Sarasota, FL). Ca^{2+} in the solution was replaced with Ba^{2+} to prevent the activation of Ca^{2+}-dependent Cl^- channels.[31,32] Recording electrodes were prepared with borosilicate glass capillary tubing using a puller (PP-830; Narishige, Tokyo, Japan); microelectrodes had a resistance of 1 to 3 MΩ when filled with 3 mol/L KCl. Whole-cell voltage clamp was achieved using these two electrodes with a Warner Instruments model OC-725C system (Warner, Hamden, CT) at –70 mV. Local anesthetics, BBG, and ATP disodium salt stocks were prepared and diluted before adding to the bath solution. AZ11645373 stocks were prepared in dimethylsulfoxide and diluted in bath solution to a final dimethylsulfoxide concentration not exceeding 0.05%. We measured the peak of the transient inward current in response to ATP that was applied for 20 seconds. Local anesthetics were preapplied for 2 minutes to allow a complete change of bath solution.

To characterize the inhibitory effect of lidocaine on P2X7 receptors, we measured ATP-induced currents at 10 μmol/L to 5 mmol/L in the presence or absence of 300 μmol/L lidocaine. The quaternary local anesthetic QX-314, which is 99.9% permanently charged and does not penetrate the cell membrane, was either injected directly into oocytes or applied outside the cell to identify whether it acts intracellularly or extracellularly. QX-314 (50 nL of 5 mmol/L diluted in 150 mmol/L KCl) was injected into oocytes to result in an intracellular concentration of approximately 500 μmol/L although, in practice, the intracellular concentration in each oocyte may be variable because the oocytes are heavily compartmentalized. Control cells were injected with 150 mmol/L KCl. Recordings were performed 10 minutes after injection. To investigate the potential use-dependent effects of lidocaine, ATP was applied at 5-minute intervals in the continuous presence of 100 μmol/L lidocaine for 30 minutes. The results are expressed as percentages of control responses.

Statistical Analyses

GraphPad Prism software (GraphPad Software, San Diego, CA) was used to conduct the statistical analysis. All values are presented as means ± SEM. The *n* values refer to the number of oocytes examined. Each experiment was performed with oocytes from at least two frogs.

The concentration–response curves for the ATP-induced peak current were fitted using the logistic function: $I = I_{min} + (I_{max} - I_{min})/[1 + (EC_{50}/A)^n]$, where I is the response induced by ATP concentration, I_{min} is the minimal response, I_{max} is the maximal response, EC_{50} is the half maximal effective concentration, A is the concentration of ATP, and n is the Hill coefficient. Differences were evaluated statistically using unpaired, two-tailed t test and one-way analysis of variance followed by Dunnett multiple comparison test, where the objective is to identify groups whose means are significantly different from the mean of a selected "reference group," in our case, no treatment with local anesthetics, or Tukey multiple comparison test, where the mean of each group is compared with the mean of every other group. Hill coefficient, half maximal inhibitory concentration (IC_{50}), and EC_{50} values were also calculated. Values of $P < 0.01$ were taken as showing a significant difference.

RESULTS

Effects of Lidocaine on Peak ATP-Induced Inward Currents in the P2X3, P2X4, and P2X7 Receptors

We determined the ATP concentration–response relation under our experimental conditions for P2X3, P2X4, and P2X7 receptors. Nonlinear regression analyses of the curves yielded the EC_{50} for ATP and slope variables (Hill coefficient) of 2.3 ± 0.8 μmol/L and 0.74 ± 0.1 in oocytes expressing P2X3 receptors, 10.8 ± 3.3 μmol/L and 0.69 ± 0.2 in oocytes expressing P2X4 receptors, and 1.2 ± 0.1 mmol/L and 3.7 ± 0.9 in oocytes expressing P2X7 receptors, respectively (Fig. 1). Based on these results, the effects of lidocaine on ATP-induced currents were examined at an ATP concentration of 2 μmol/L for P2X3 receptor, 10 μmol/L for P2X4 receptor, and 1 mmol/L for P2X7 receptor. Figure 2B shows concentration–response relations of lidocaine-mediated inhibition on ATP-induced currents in three receptors. Lidocaine inhibited the currents in a concentration-dependent manner in oocytes expressing P2X7 receptor; the IC_{50} value of lidocaine for ATP-induced currents and the slope were 282 ± 45 μmol/L and 0.72 ± 0.07, respectively (Table 1). These inhibitory effects were significant at concentrations of lidocaine ≥30 μmol/L (Fig. 2B). By contrast, the inhibitory effects of lidocaine on the P2X3 and P2X4 receptors were limited. Specifically, only a high concentration of 10 mmol/L lidocaine significantly suppressed ATP-induced currents to 68 ± 6% and 71 ± 6% of the control in oocytes expressing P2X3 and P2X4 receptors, respectively (Fig. 2B).

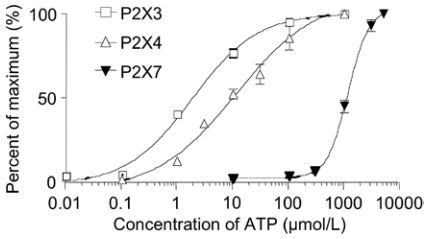

Figure 1. Concentration–response curves for adenosine triphosphate (ATP)-induced currents in *Xenopus* oocytes expressing P2X3, P2X4, and P2X7 receptors. Oocytes were voltage clamped at −70 mV. ATP (10 nmol/L to 1 mmol/L for P2X3; 100 nmol/L to 1 mmol/L for P2X4; and 10 μmol/L to 5 mmol/L for P2X7) was applied for 20 seconds, and peak current was measured. Values are the mean ± SEM (n = 6).

Effects of Other Local Anesthetics on the P2X7 Receptor

We next examined the effects of other local anesthetics including mepivacaine, ropivacaine, and bupivacaine on ATP-induced currents in oocytes expressing P2X7 receptor because lidocaine inhibited this receptor most strongly. Although mepivacaine suppressed ATP-induced currents in a concentration-dependent manner, the inhibitory effects were less than those of lidocaine with the IC_{50} value and slope variable of 6.0 ± 0.06 mmol/L and 0.62 ± 0.06, respectively. This suggests that the inhibitory potency of mepivacaine was one-twentieth of that of lidocaine (Fig. 3, Table 1). By contrast, ropivacaine and bupivacaine had little effect on ATP-induced currents (Fig. 3).

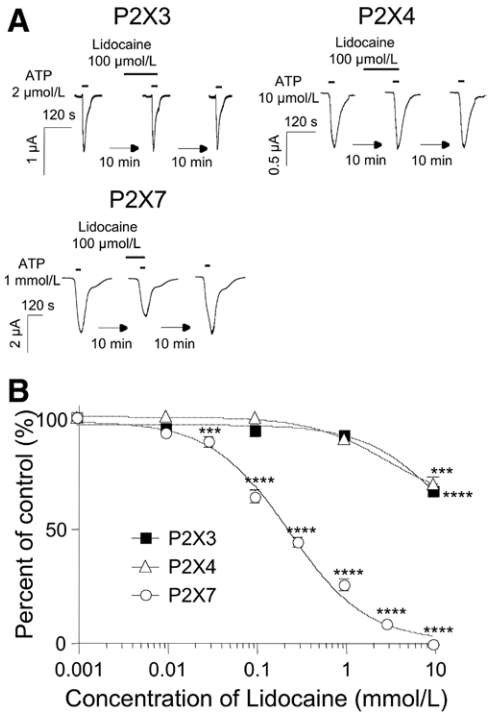

Figure 2. Effects of lidocaine on the adenosine triphosphate (ATP)-induced currents in *Xenopus* oocytes expressing P2X3, P2X4, and P2X7 receptors. A, Representative traces from oocytes expressing P2X3, P2X4, and P2X7 receptors in both the absence and presence of 100 μmol/L lidocaine. P2X3, P2X4, and P2X7 receptors were activated by 2 μmol/L, 10 μmol/L, and 1 mmol/L of ATP, respectively. ATP was applied for 20 seconds with or without pretreatment for 2 minutes with 100 μmol/L lidocaine. The currents of lidocaine-treated oocytes were recorded 10 minutes after recording the control currents, and the washout currents were obtained 10 minutes after lidocaine treatment. B, Concentration–response curves for the inhibitory effects of lidocaine on ATP-induced currents in P2X3, P2X4, and P2X7 receptors. The peak current amplitude in the presence of lidocaine was normalized to that of the control and the effects are expressed as percentages of the control. Lidocaine inhibited ATP-induced currents in oocytes expressing both P2X3 and P2X4 receptors at only a high concentration of 10 mmol/L. In contrast, lidocaine suppressed ATP-induced currents in oocytes expressing P2X7 concentration dependently, and it reduced those currents to 93 ± 4%, 89 ± 5%, 65 ± 8%, 45 ± 6%, 26 ± 7%, and 9 ± 2% of control at 10 μmol/L, 30 μmol/L, 100 μmol/L, 300 μmol/L, 1 mmol/L, and 3 mmol/L, respectively. Data are presented as means ± SEM (n = 6). Hill coefficient and half maximal inhibitory concentration (IC_{50}) values were calculated using GraphPad Prism. ***$P < 0.001$ and ****$P < 0.0001$ compared with the control (one-way analysis of variance followed by Dunnett post hoc test).

Table 1. Effects of Lidocaine, Mepivacaine, QX-314, and Benzocaine on IC_{50} Value and Hill Coefficient Calculated from the Concentration–Response Curves Shown in Figures 3 and 5

	Lidocaine	Mepivacaine	QX-314	Benzocaine
IC_{50} (μmol/L)	282 ± 45	6020 ± 61	500 ± 75	1560 ± 39
Hill coefficient	0.72 ± 0.07	0.62 ± 0.06	0.36 ± 0.03	0.88 ± 0.07

IC_{50} = half maximal inhibitory concentration; QX-314 = (*N*-[2,6-dimethylphenylcarbamoylmethyl] triethylammonium bromide).

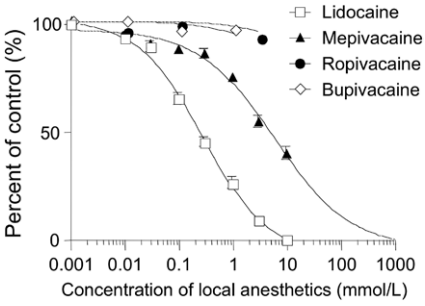

Figure 3. Concentration–response curves for inhibitory effects of local anesthetics including lidocaine, mepivacaine, ropivacaine, and bupivacaine on adenosine triphosphate–induced currents in P2X7 receptors. The peak current amplitude in the presence of local anesthetics was normalized to that of the control and the effects are expressed as percentages of the control. Data are presented as means ± SEM (n = 6). Hill coefficient and half maximal inhibitory concentration (IC_{50}) values were calculated using GraphPad Prism.

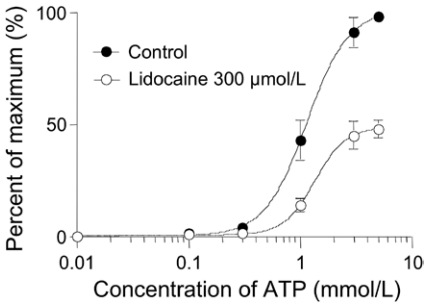

Figure 4. Characterization of the inhibitory effects of lidocaine on adenosine triphosphate (ATP)-induced currents in oocytes expressing P2X7 receptor. We measured the currents induced by 10 μmol/L to 5 mmol/L ATP in the absence and presence of 300 μmol/L lidocaine. Lidocaine did not change the half maximal effective concentration (EC_{50}) value and the the slope variable (hill coefficient) (control, 1.2 ± 0.1 mmol/L and 3.7 ± 0.9; lidocaine, 1.4 ± 0.2 mmol/L and 4.8 ± 1.1), however, it significantly reduced the maximal response (E_{max}) value to 49 ± 4% of control (P < 0.0001; 99% confidence interval, −65.7 to −35.1). Data are presented as means ± SEM (n = 6). Hill coefficient, EC_{50}, and E_{max} values were calculated using GraphPad Prism. Data were statistically evaluated by unpaired t test (two-tailed) using the same software.

Characterization of the Inhibitory Effects of Lidocaine on the P2X7 Receptor

To determine whether lidocaine competes with ATP for the P2X7 receptor, we next investigated the effects of 300 μmol/L lidocaine on the ATP concentration–response curve. ATP-induced currents at concentrations of 10 μmol/L to 5 mmol/L were measured in the absence and presence of lidocaine. As shown in Figure 4, lidocaine-mediated inhibition was not overcome by increasing the ATP concentration. In addition, lidocaine significantly reduced the E_{max} value (maximal response) of the ATP concentration–response curve to 49% ± 4% (P < 0.0001; 99% confidence interval [CI], −65.7 to −35.1). The EC_{50} and slope variables in the absence and presence of lidocaine were 1.2 ± 0.1 mmol/L and 3.7 ± 0.9, and 1.4 ± 0.2 mmol/L and 4.8 ± 1.1, respectively. Thus, lidocaine significantly suppressed E_{max} without significantly changing EC_{50} (P = 0.385; 99% CI, −0.279 to 0.665) and slope variables (P = 0.483; 99% CI, −2.165 to 4.268), suggesting noncompetitive inhibition.

Effects of Charged and Uncharged Local Anesthetics on the P2X7 Receptor

We next assessed the effects of QX-314, which is a permanently charged and non–membrane-permeable lidocaine analog, on the P2X7 receptor. When applied extracellularly, QX-314 inhibited ATP-induced currents in a concentration-dependent manner; the IC_{50} value and slope variable were 500 ± 75 μmol/L and 0.36 ± 0.03, respectively (Fig. 5B, Table 1). Moreover, intracellular QX-314 injection also significantly suppressed ATP-activated currents to 51 ± 9% of the control, whereas injected 150 mmol/L KCl had no effect (112 ± 11% of the control) (Fig. 5C). These results suggest that QX-314 can act on the P2X7 receptor both extracellularly and intracellularly, and the charged lidocaine can suppress the function of P2X7. Therefore, we investigated whether charge is required for the inhibitory actions of local anesthetics on the P2X7 receptor by measuring the effects of benzocaine, a local anesthetic that is almost completely uncharged and highly membrane permeable. Benzocaine suppressed the response to ATP in a concentration-dependent manner with the IC_{50} value and the slope variable of 1.6 ± 0.04 mmol/L and 0.88 ± 0.07, respectively (Fig. 5B, Table 1). These data suggest that both charged and uncharged local anesthetics can suppress P2X7 receptor function although it remains unclear whether benzocaine acts intracellularly or extracellularly.

Analyzing the Use Dependency of Lidocaine-Mediated Inhibition of the P2X7 Receptor

We assessed whether the effects of lidocaine on the P2X7 receptor were use-dependent because local anesthetics exhibit use-dependent block of voltage-gated sodium channel function, ATP was applied to oocytes at 5-minute intervals in the absence or continuous presence of 100 μmol/L lidocaine for 30 minutes (Fig. 6A). In the continuous presence of lidocaine, the response to the second application of ATP (after 5 minutes) was significantly reduced to 66 ± 3% of the current induced by the first application (0 minute), and the inhibitory effect of the seventh application (30 minutes) was similar to that of the second application (5 minutes) (Fig. 6, B and C). Therefore, these results revealed the effectiveness of lidocaine as it reached steady state in the second application of ATP (5 minutes), suggesting that lidocaine-mediated inhibition of the P2X7 receptor is use-dependent. More potent inhibition might be observed in the second application compared with the first because lidocaine would be able to access its site of

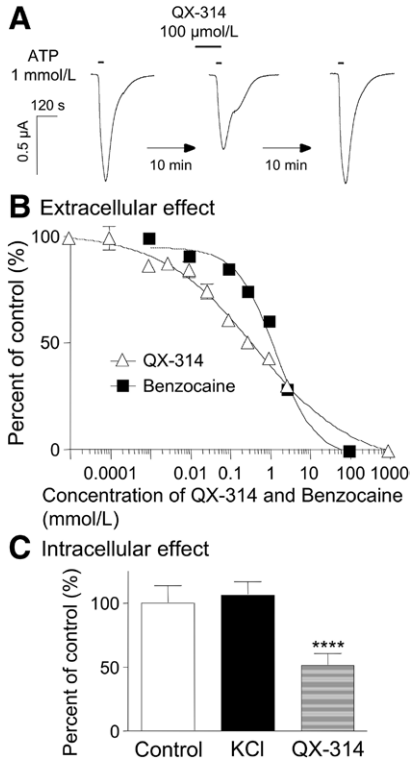

Figure 5. Effects of *N*-(2,6-dimethylphenylcarbamoylmethyl) triethylammonium bromide (QX-314) and benzocaine on adenosine triphosphate (ATP)-induced currents in oocytes expressing P2X7 receptor. A, Representative traces from oocytes expressing P2X7 receptors in both the absence and presence of extracellular 100 μmol/L QX-314. ATP was applied for 20 seconds with or without pretreatment for 2 minutes with 100 μmol/L QX-314. The currents of QX-314-treated oocytes were recorded 10 minutes after recording the control currents, and the washout currents were obtained 10 minutes after QX-314 treatment. B, Concentration–response curves for extracellular QX-314 and benzocaine-mediated inhibition on ATP-induced currents in oocytes expressing P2X7 receptors. The peak current amplitude in the presence of local anesthetics was normalized to that of the control, and the effects are expressed as percentages of the control. QX-314 and benzocaine reduced ATP-induced currents in a concentration-dependent manner with the half maximal inhibitory concentration (IC_{50}) values and slope variables of 500 ± 75 μmol/L and 0.36 ± 0.03, and 1.6 ± 0.04 mmol/L and 0.88 ± 0.07, respectively. C, Effects of intracellular QX-314 on ATP-induced currents in oocytes expressing P2X7 receptor. ATP-induced currents were recorded 10 minutes after intracellular injection of 5 mmol/L QX-314 diluted by 150 mmol/L potassium chloride (KCl), resulting in intracellular concentration of 500 μmol/L and intracellular injection of 150 mmol/L KCl as control cells. Intracellular injection of QX-314 significantly suppressed ATP-induced currents to 51 ± 9% of control although that of 150 mmol/L KCl did not reduce those currents. Data are presented as means ± SEM (n = 6). Hill coefficient and IC_{50} values were calculated using GraphPad Prism. ****P < 0.0001 compared with the control (one-way analysis of variance followed by Dunnett post hoc test).

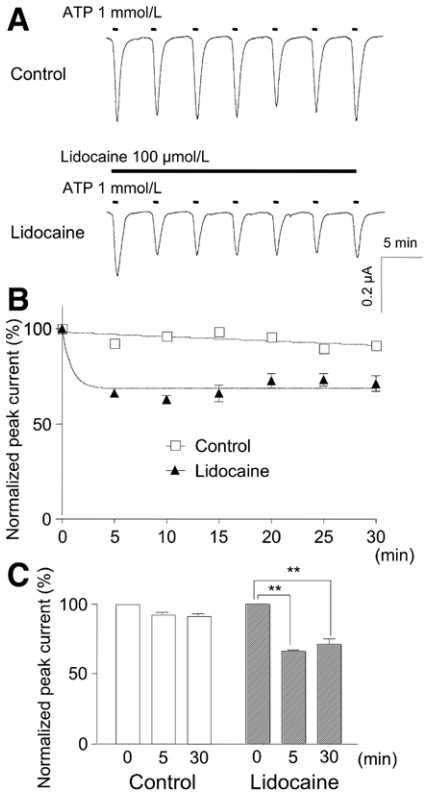

Figure 6. Analyses of use dependency of lidocaine block on P2X7 receptor. Repetitive application of 1 mmol/L adenosine triphosphate (ATP; 20 seconds) at 5-minute intervals was done in the absence or continuous presence of 100 μmol/L lidocaine for 30 minutes. A, Representative traces induced by repetitive ATP application for 30 minutes from oocytes expressing P2X7 receptors in the absence or continuous presence of 100 μmol/L lidocaine. All typical traces were obtained from the same oocyte. B, Peak currents were normalized to the first pulse and plotted against the pulse number. C, Comparison of the normalized currents between the first (0 minute), second (5 minutes), and seventh (30 minutes) applications. In the continuous presence of lidocaine, the responses to the second application of ATP (5 minutes) were significantly reduced to 66% ± 3% of currents induced by the first application of ATP (0 minute). However, inhibitory effect at seventh application (30 minutes) was statistically the same as that at second application (5 minutes). Data are expressed as means ± SEM (n = 6). **P < 0.01 compared with the control (one-way analysis of variance followed by Tukey post hoc test).

action sufficiently during a 5-minute treatment, whereas the first application in which lidocaine and ATP were simultaneously applied (no lidocaine pretreatment) would not be sufficient for lidocaine to access its site of action.

Effects of Selective P2X7 Receptor Antagonists on the Inhibitory Actions of Lidocaine

We next investigated the action of lidocaine in the absence and presence of selective antagonists of the P2X7 receptor, BBG, or AZ11645373 to determine whether these compounds modulate the inhibitory actions of lidocaine on the P2X7 receptor. Oocytes were pretreated with 1 μmol/L BBG or 300 nmol/L AZ11645373 2 minutes before coapplication of 10 μmol/L to 3 mmol/L lidocaine for 2 minutes (Fig. 7, A and B). Figure 7, C and D, shows normalized inhibition curves for lidocaine in the absence and presence of preapplied and coapplied BBG or AZ11645373. The IC_{50} values and slope variables of the lidocaine concentration–response curves with BBG or AZ11645373 were 315 ± 56 μmol/L and 0.92 ± 0.14, or 258 ± 52 μmol/L and 0.93 ± 0.18, respectively. This suggests that neither BBG nor AZ11645373 modulated the effects of lidocaine, which exhibited an IC_{50} value and slope variable of 282 ± 45 μmol/L and 0.72 ± 0.07, respectively (P = 0.658 and 0.237, or P = 0.736 and 0.309, respectively, for the IC_{50} values and the slope variables of the lidocaine concentration–response curves with BBG or AZ11645373, 99% CI, −132.7 to 198.7 and −0.161 to 0.561, or −134.6 to 182.6 and

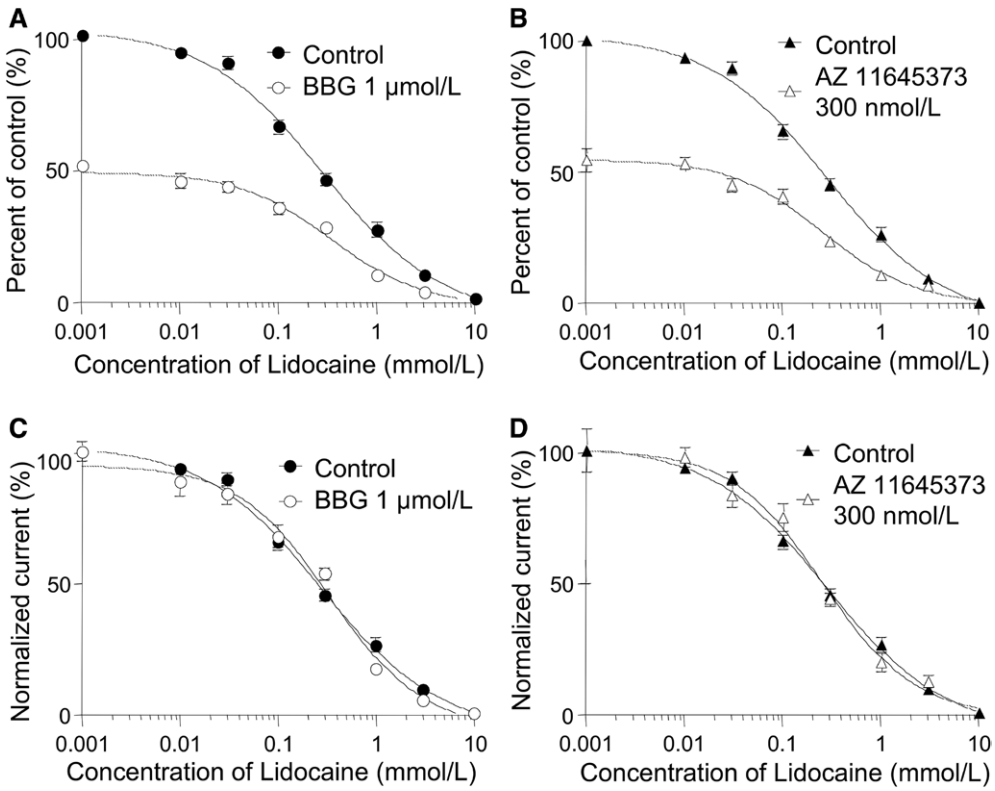

Figure 7. Consentration-response curves for lidocaine inhibition in the absence or presence of pre-treatment for 4-min by 1 μmol/L BBG (A) or 300 nmol/L AZ11645373 (B). BBG or AZ11645373 were pre-applied for 2 min prior to co-application with lidocaine (10 μmol/L–3 mmol/L) for 2 min. Normalized inhibition curves for lidocaine in the absence and presence of BBG (C) or AZ11645373 (D) were obtained from (A) and (B). Both BBG and AZ11645373 did not affect inhibitory effect of lidocaine on P2X7 receptor; the IC50 values and slope variables were 282 ± 45 μmol/L and 0.72 ± 0.07, 315 ± 56 μmol/L and 0.92 ± 0.14, and 258 ± 52 μmol/L and 0.93 ± 0.18, in control, BBG, and AZ11645373 pre-treatment, respectively. Data are expressed as means ± SEM (n = 6). Hill coefficient, IC50 values were calculated using GraphPad Prism. ATP = adenosine triphosphate; BBG = Brilliant Blue G; IC50 = half maximal inhibitory concentration.

−0.235 to 0.655). Overall, these data suggest that lidocaine interacts with a different site on the P2X7 receptor from the sites of action of either BBG or AZ11645373, which are noncompetitive antagonists of the P2X7 receptor.

DISCUSSION

In the present study, we demonstrated that lidocaine selectively inhibited ATP-induced inward currents of the P2X7 receptor in a concentration-dependent manner. To our knowledge, this study is the first direct evidence that lidocaine suppresses the P2X7 receptor. Substantial pain relief is achieved at plasma concentrations of 2 to 5 μg/mL (7–20 μmol/L) by continuous infusion of lidocaine in cancer patients with neuropathic pain.[33] In the present study, the IC_{50} value of lidocaine-mediated P2X7 inhibition was 282 ± 45 μmol/L. Lidocaine tended to suppress ATP-induced currents at concentrations ≥10 μmol/L, and these inhibitory effects were significant at concentrations ≥30 μmol/L ($P <$ 0.001). Although it is not proven whether a small inhibitory effect (7% inhibition) of lidocaine at 10 μmol/L produces pain relief in systemic administration, lidocaine might suppress P2X7 function at least when it is administered locally such as epidural administration because P2X7 receptors are expressed on glial cells in spinal neurons.

Lidocaine had little effect on the P2X3 and P2X4 receptors, but selectively suppressed the function of P2X7 receptors. The P2X7 receptor is structurally distinct from other P2X receptors; it also has different gating properties although these are only poorly understood.[34] The P2X7 receptor is permeable not only to small cations (sodium, potassium, and calcium) as similar to other subunits but also to larger cations such as *N*-methyl-D-glucamine and nanometer-sized dyes,[35] probably through the progressive dilation of the pore or the opening of a distinct accessory channel.[36] Therefore, it is of great interest to explore how lidocaine inhibits the function of the P2X7 receptor alone. Lidocaine would not affect three ATP-binding sites that are shown to exist in the extracellular region of P2X receptors[37] because lidocaine-mediated inhibition was found to be noncompetitive in this study. Moreover, lidocaine-mediated inhibition of the P2X7 receptor was use-dependent. Taken together, these findings suggest that lidocaine exerts its effects by affecting the site in the ion channel pore. By contrast, the inhibitory effects of QX-314 and benzocaine suggest that both charged and uncharged local anesthetics can also suppress P2X7 function. Moreover, intracellular injection of the charged local anesthetic QX-314 also inhibited P2X7 function. These results suggest that lidocaine acts on both intracellular and extracellular sites of the P2X7 receptor and that both charged and uncharged lidocaine could modulate this receptor.

We demonstrated that other local anesthetics including mepivacaine, ropivacaine, and bupivacaine have only limited effects on P2X7 receptor function. All these three

compounds, but not lidocaine, contain a piperidine ring (Fig. 8), to which is attached a carbon chain of different lengths; one carbon in mepivacaine, three in ropivacaine, and four in bupivacaine. Therefore, it is possible that the piperidine ring is an obstacle to the action of local anesthetics because the inhibitory potency of mepivacaine was one-twentieth of that of lidocaine. Moreover, longer carbon chains connected to the piperidine ring may further hinder potential effects because both ropivacaine and bupivacaine had little effect on the P2X7 receptor. Therefore, it is possible that lidocaine suppresses P2X7 receptor function by acting on a binding site in the ion channel. Recent X-ray crystal structural analyses of P2X4 receptor in zebrafish revealed that P2X receptors exhibit homotrimeric architecture and that each subunit consists of a large hydrophilic extracellular domain and a transmembrane domain composed of two α-helices, which resemble the shape of a dolphin.[38,39] These analyses also revealed that binding of ATP to the ATP-binding pocket within an intersubunit cleft rotates each subunit, resulting in promotion of the ion channel pore opening. P2X3, P2X4, and P2X7 are 40% to 50% identical in amino acid sequence, and each subunit of the P2X7 receptor has a longer amino acid sequence (595) than P2X3 (397) and P2X4 (388) because only P2X7 has a long intracellular C-terminus. Therefore, lidocaine might bind to the binding pocket for local anesthetics that exists mainly in the P2X7 receptor because of the differences of amino acid sequence to prevent the subunits from rotating that leads to channel opening.

Many P2X7 receptor antagonists have been reported in addition to antagonists of other P2X receptor subunits although they are not used clinically.[34] Some antagonists, including pyridoxal phosphate-6-azophenyl-2′,4′-disulfonic acid and periodate-oxidized ATP, were demonstrated to interact at the ATP-binding sites, showing that they were competitive antagonists.[40] By contrast, many of them inhibit P2X7-mediated responses by acting in a noncompetitive manner. We examined whether BBG and AZ11645373 interact with the inhibitory action of lidocaine on P2X7 receptors because these two compounds are selective P2X7 inhibitors and act in a similar noncompetitive manner to lidocaine. BBG was shown to produce a noncompetitive inhibition of rat P2X7 receptors more potently than human P2X7 receptors; IC_{50} values were 10 and 200 nmol/L, respectively,[41] whereas

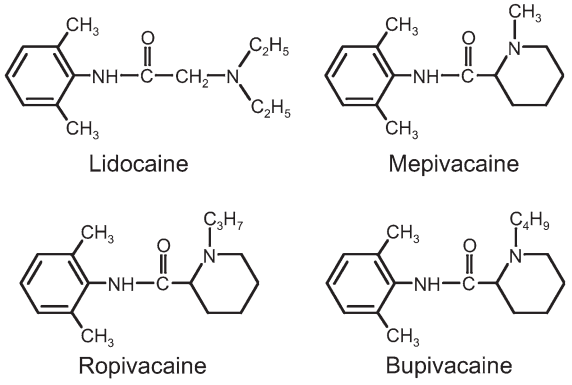

Figure 8. Structures of lidocaine, mepivacaine, ropivacaine, and bupivacaine.

it was reported that AZ11645373 is a highly selective and potent antagonist at human, but not at rat, P2X7 receptors.[42] Our data suggested that lidocaine acts on a different site of the P2X7 receptor than both BBG and AZ11645373.

The systemic administration of lidocaine has been considered to reduce neuropathic pain via suppression of ectopic activity by inhibiting abnormally expressed voltage-gated sodium channels.[5] One study demonstrated that the incidence of C-fibers with ongoing activity was significantly reduced by systemic administration of lidocaine resulting in low plasma concentrations in a chronic inflammatory model.[43] However, it was also shown that this effect was only partially correlated with chronic pain relief compared with the complete inhibition of spontaneous discharge in C-fibers, suggesting that there may be mechanisms other than blocking sodium channel activity. Moreover, many reports demonstrate that lidocaine also affects other pain signaling pathways.[6] It has been demonstrated that intravenous lidocaine infusion increased acetylcholine concentrations in cerebrospinal fluid, which exacerbated inhibitory descending pain pathways resulting in analgesia.[44] Lidocaine has also been shown to produce central inhibitory effects via spinal strychnine-sensitive glycine receptors[45] and to stimulate the release of endogenous opioids to promote its analgesic effect.[46] Moreover, lidocaine has been reported to reduce the postsynaptic depolarization mediated by *N*-methyl-D-aspartate and neurokinin receptors,[47] and a study in a recombinant model demonstrated that local anesthetics, including lidocaine, directly inhibited the activation of human *N*-methyl-D-aspartate receptors in a concentration-dependent manner.[48]

The P2X7 receptor is expressed predominantly on immune cells and has been shown to play an important role in the inflammatory response by demonstrating that activation of the P2X7 receptor leads to maturation and release of interleukin (IL)-1β and initiation of a cytokine cascade.[49,50] Several reports also suggest a role for the P2X7 receptor in pain modulation because systemic administration of selective antagonists of P2X7 receptors produced antinociceptive effects,[51] and hypersensitivity was not observed in P2X7-knockout mice[52] in neuropathic and inflammatory pain models. In addition, some reports suggest that lidocaine exerts anti-inflammatory effects by suppressing cytokine-induced injury[53] or attenuating the production of proinflammatory cytokines including tumor necrosis factor-α, IL-1β, and IL-6 induced by extracellular ATP in microglia.[54] Taken together, these data indicate that P2X7 receptor antagonists might be beneficial for the treatment of neuropathic and inflammatory pain. Therefore, suppression of the P2X7 receptor might be a mechanism underlying the anti-inflammatory effects and chronic pain relief affected by lidocaine. Although our present results suggest that the P2X3 and P2X4 receptors are not involved in the mechanism of lidocaine-induced pain relief, further experiments are needed to investigate the effects on other subunits including P2X2/3 or P2Y12, which are also related to chronic pain. Although ropivacaine and bupivacaine can relieve neuropathic pain effectively by epidural administration, P2X7 signaling would not be involved in their mechanism underlying pain relief.

In conclusion, lidocaine selectively inhibited ATP-induced currents of P2X7 receptors expressed in *Xenopus*

oocytes at clinically relevant concentrations when it was administered locally at least. The effect of lidocaine on P2X7 receptors was likely a result of noncompetitive inhibition at both extracellular and intracellular sites in the ion channel pore. To our knowledge, these results are the first evidence showing novel lidocaine-mediated effects on P2X receptors in a recombinant experimental system and might become the key to elucidate the mechanisms of pain relief by lidocaine. However, further studies are needed to clarify the relevance of P2X7 receptor inhibition of the analgesic effects of lidocaine.

DISCLOSURES

Name: Dan Okura, MD.
Contribution: This author conducted data collection, data analysis, and manuscript preparation.
Attestation: Dan Okura approved the final manuscript, and attests to the integrity of the original data and the analysis reported in this manuscript.
Name: Takafumi Horishita, MD, PhD.
Contribution: This author helped study design, data collection, data analysis, and manuscript preparation.
Attestation: Takafumi Horishita approved the final manuscript, attests to the integrity of the original data and the analysis reported in this manuscript and also is the archival author.
Name: Susumu Ueno, MD, PhD.
Contribution: This author helped design the study, and prepare the manuscript.
Attestation: Susumu Ueno approved the final manuscript.
Name: Nobuyuki Yanagihara, PhD.
Contribution: This author helped prepared the manuscript.
Attestation: Nobuyuki Yanagihara approved the final manuscript.
Name: Yuka Sudo, PhD.
Contribution: This author helped prepare the manuscript.
Attestation: Yuka Sudo approved the final manuscript.
Name: Yasuhito Uezono, MD, PhD.
Contribution: This author helped prepare the manuscript.
Attestation: Yasuhito Uezono approved the final manuscript.
Name: Tomoko Minami, MD.
Contribution: This author helped prepare the manuscript.
Attestation: Tomoko Minami approved the final manuscript.
Name: Takashi Kawasaki, MD, PhD.
Contribution: This author helped prepare the manuscript.
Attestation: Takashi Kawasaki approved the final manuscript.
Name: Takeyoshi Sata, MD, PhD.
Contribution: This author helped conduct the study and prepare the manuscript.
Attestation: Takeyoshi Sata approved the final manuscript.
This manuscript was handled by: Markus W. Hollmann, MD, PhD, DEAA.

REFERENCES

1. Mao J, Chen LL. Systemic lidocaine for neuropathic pain relief. Pain 2000;87:7–17
2. Buchanan DD, J MacIvor F. A role for intravenous lidocaine in severe cancer-related neuropathic pain at the end-of-life. Support Care Cancer 2010;18:899–901
3. Lai J, Hunter JC, Porreca F. The role of voltage-gated sodium channels in neuropathic pain. Curr Opin Neurobiol 2003;13: 291–7
4. Baron R, Binder A, Wasner G. Neuropathic pain: diagnosis, pathophysiological mechanisms, and treatment. Lancet Neurol 2010;9:807–19
5. Amir R, Argoff CE, Bennett GJ, Cummins TR, Durieux ME, Gerner P, Gold MS, Porreca F, Strichartz GR. The role of sodium channels in chronic inflammatory and neuropathic pain. J Pain 2006;7:S1–29
6. Groudine SB, Fisher HA, Kaufman RP Jr, Patel MK, Wilkins LJ, Mehta SA, Lumb PD. Intravenous lidocaine speeds the return of bowel function, decreases postoperative pain, and shortens hospital stay in patients undergoing radical retropubic prostatectomy. Anesth Analg 1998;86:235–9
7. Cooke ED, Bowcock SA, Lloyd MJ, Pilcher MF. Intravenous lignocaine in prevention of deep venous thrombosis after elective hip surgery. Lancet 1977;2:797–9
8. Hollmann MW, Durieux ME. Local anesthetics and the inflammatory response: a new therapeutic indication? Anesthesiology 2000;93:858–75
9. Jänig W. What is the mechanism underlying treatment of pain by systemic application of lidocaine? Pain 2008;137:5–6
10. Hollmann MW, McIntire WE, Garrison JC, Durieux ME. Inhibition of mammalian Gq protein function by local anesthetics. Anesthesiology 2002;97:1451–7
11. Bräu ME, Nau C, Hempelmann G, Vogel W. Local anesthetics potently block a potential insensitive potassium channel in myelinated nerve. J Gen Physiol 1995;105:485–505
12. Xiong Z, Strichartz GR. Inhibition by local anesthetics of Ca^{2+} channels in rat anterior pituitary cells. Eur J Pharmacol 1998;363:81–90
13. North RA. Molecular physiology of P2X receptors. Physiol Rev 2002;82:1013–67
14. Lang PM, Sippel W, Schmidbauer S, Irnich D, Grafe P. Functional evidence for P2X receptors in isolated human vagus nerve. Anesthesiology 2003;99:232–5
15. Burnstock G, Knight GE. Cellular distribution and functions of P2 receptor subtypes in different systems. Int Rev Cytol 2004;240:31–304
16. Khakh BS, North RA. P2X receptors as cell-surface ATP sensors in health and disease. Nature 2006;442:527–32
17. Burnstock G. Pathophysiology and therapeutic potential of purinergic signaling. Pharmacol Rev 2006;58:58–86
18. Eltzschig HK, Sitkovsky MV, Robson SC. Purinergic signaling during inflammation. N Engl J Med 2012;367:2322–33
19. Eltzschig HK. Targeting purinergic signaling for perioperative organ protection. Anesthesiology 2013;118:1001–4
20. Gum RJ, Wakefield B, Jarvis MF. P2X receptor antagonists for pain management: examination of binding and physicochemical properties. Purinergic Signal 2012;8:41–56
21. Honore P, Kage K, Mikusa J, Watt AT, Johnston JF, Wyatt JR, Faltynek CR, Jarvis MF, Lynch K. Analgesic profile of intrathecal P2X(3) antisense oligonucleotide treatment in chronic inflammatory and neuropathic pain states in rats. Pain 2002;99:11–9
22. Tsuda M, Shigemoto-Mogami Y, Koizumi S, Mizokoshi A, Kohsaka S, Salter MW, Inoue K. P2X4 receptors induced in spinal microglia gate tactile allodynia after nerve injury. Nature 2003;424:778–83
23. Chessell IP, Hatcher JP, Bountra C, Michel AD, Hughes JP, Green P, Egerton J, Murfin M, Richardson J, Peck WL, Grahames CB, Casula MA, Yiangou Y, Birch R, Anand P, Buell GN. Disruption of the P2X7 purinoceptor gene abolishes chronic inflammatory and neuropathic pain. Pain 2005;114:386–96
24. Andoh T, Furuya R, Oka K, Hattori S, Watanabe I, Kamiya Y, Okumura F. Differential effects of thiopental on neuronal nicotinic acetylcholine receptors and P2X purinergic receptors in PC12 cells. Anesthesiology 1997;87:1199–209
25. Furuya R, Oka K, Watanabe I, Kamiya Y, Itoh H, Andoh T. The effects of ketamine and propofol on neuronal nicotinic acetylcholine receptors and P2x purinoceptors in PC12 cells. Anesth Analg 1999;88:174–80
26. Nakanishi M, Mori T, Nishikawa K, Sawada M, Kuno M, Asada A. The effects of general anesthetics on P2X7 and P2Y receptors in a rat microglial cell line. Anesth Analg 2007;104:1136–44
27. Xiong K, Hu XQ, Stewart RR, Weight FF, Li C. The mechanism by which ethanol inhibits rat P2X4 receptors is altered by mutation of histidine 241. Br J Pharmacol 2005;145:576–86
28. Nagata K, Imai T, Yamashita T, Tsuda M, Tozaki-Saitoh H, Inoue K. Antidepressants inhibit P2X4 receptor function: a

possible involvement in neuropathic pain relief. Mol Pain 2009;5:20
29. Horishita T, Eger EI II, Harris RA. The effects of volatile aromatic anesthetics on voltage-gated Na^+ channels expressed in *Xenopus* oocytes. Anesth Analg 2008;107:1579–86
30. Okura D, Horishita T, Ueno S, Yanagihara N, Sudo Y, Uezono Y, Sata T. The endocannabinoid anandamide inhibits voltage-gated sodium channels Nav1.2, Nav1.6, Nav1.7, and Nav1.8 in *Xenopus* oocytes. Anesth Analg 2014;118:554–62
31. Khakh BS, Bao XR, Labarca C, Lester HA. Neuronal P2X transmitter-gated cation channels change their ion selectivity in seconds. Nat Neurosci 1999;2:322–30
32. Roberts JA, Digby HR, Kara M, El Ajouz S, Sutcliffe MJ, Evans RJ. Cysteine substitution mutagenesis and the effects of methanethiosulfonate reagents at P2X2 and P2X4 receptors support a core common mode of ATP action at P2X receptors. J Biol Chem 2008;283:20126–36
33. Devulder JE, Ghys L, Dhondt W, Rolly G. Neuropathic pain in a cancer patient responding to subcutaneously administered lignocaine. Clin J Pain 1993;9:220–3
34. Coddou C, Yan Z, Obsil T, Huidobro-Toro JP, Stojilkovic SS. Activation and regulation of purinergic P2X receptor channels. Pharmacol Rev 2011;63:641–83
35. Browne LE, Compan V, Bragg L, North RA. P2X7 receptor channels allow direct permeation of nanometer-sized dyes. J Neurosci 2013;33:3557–66
36. Becker D, Woltersdorf R, Boldt W, Schmitz S, Braam U, Schmalzing G, Markwardt F. The P2X7 carboxyl tail is a regulatory module of P2X7 receptor channel activity. J Biol Chem 2008;283:25725–34
37. Browne LE, Jiang LH, North RA. New structure enlivens interest in P2X receptors. Trends Pharmacol Sci 2010;31:229–37
38. Kawate T, Michel JC, Birdsong WT, Gouaux E. Crystal structure of the ATP-gated P2X(4) ion channel in the closed state. Nature 2009;460:592–8
39. Hattori M, Gouaux E. Molecular mechanism of ATP binding and ion channel activation in P2X receptors. Nature 2012;485:207–12
40. Michel AD, Xing M, Thompson KM, Jones CA, Humphrey PP. Decavanadate, a P2X receptor antagonist, and its use to study ligand interactions with P2X7 receptors. Eur J Pharmacol 2006;534:19–29
41. Jiang LH, Mackenzie AB, North RA, Surprenant A. Brilliant blue G selectively blocks ATP-gated rat P2X(7) receptors. Mol Pharmacol 2000;58:82–8
42. Stokes L, Jiang LH, Alcaraz L, Bent J, Bowers K, Fagura M, Furber M, Mortimore M, Lawson M, Theaker J, Laurent C, Braddock M, Surprenant A. Characterization of a selective and potent antagonist of human P2X(7) receptors, AZ11645373. Br J Pharmacol 2006;149:880–7
43. Xiao WH, Bennett GJ. C-fiber spontaneous discharge evoked by chronic inflammation is suppressed by a long-term infusion of lidocaine yielding nanogram per milliliter plasma levels. Pain 2008;137:218–28
44. Abelson KS, Höglund AU. Intravenously administered lidocaine in therapeutic doses increases the intraspinal release of acetylcholine in rats. Neurosci Lett 2002;317:93–6
45. Biella G, Sotgiu ML. Central effects of systemic lidocaine mediated by glycine spinal receptors: an iontophoretic study in the rat spinal cord. Brain Res 1993;603:201–6
46. Cohen SP, Mao J. Is the analgesic effect of systemic lidocaine mediated through opioid receptors? Acta Anaesthesiol Scand 2003;47:910–1
47. Nagy I, Woolf CJ. Lignocaine selectively reduces C fibre-evoked neuronal activity in rat spinal cord in vitro by decreasing *N*-methyl-D-aspartate and neurokinin receptor-mediated postsynaptic depolarizations; implications for the development of novel centrally acting analgesics. Pain 1996;64:59–70
48. Hahnenkamp K, Durieux ME, Hahnenkamp A, Schauerte SK, Hoenemann CW, Vegh V, Theilmeier G, Hollmann MW. Local anaesthetics inhibit signalling of human NMDA receptors recombinantly expressed in *Xenopus laevis* oocytes: role of protein kinase C. Br J Anaesth 2006;96:77–87
49. Solle M, Labasi J, Perregaux DG, Stam E, Petrushova N, Koller BH, Griffiths RJ, Gabel CA. Altered cytokine production in mice lacking P2X(7) receptors. J Biol Chem 2001;276:125–32
50. Ferrari D, Pizzirani C, Adinolfi E, Lemoli RM, Curti A, Idzko M, Panther E, Di Virgilio F. The P2X7 receptor: a key player in IL-1 processing and release. J Immunol 2006;176:3877–83
51. Donnelly-Roberts DL, Jarvis MF. Discovery of P2X7 receptor-selective antagonists offers new insights into P2X7 receptor function and indicates a role in chronic pain states. Br J Pharmacol 2007;151:571–9
52. Clark AK, Staniland AA, Marchand F, Kaan TK, McMahon SB, Malcangio M. P2X7-dependent release of interleukin-1beta and nociception in the spinal cord following lipopolysaccharide. J Neurosci 2010;30:573–82
53. de Klaver MJ, Buckingham MG, Rich GF. Lidocaine attenuates cytokine-induced cell injury in endothelial and vascular smooth muscle cells. Anesth Analg 2003;97:465–70
54. Su D, Gu Y, Wang Z, Wang X. Lidocaine attenuates proinflammatory cytokine production induced by extracellular adenosine triphosphate in cultured rat microglia. Anesth Analg 2010;111:768–74

A cross-fostering analysis of bromine ion concentration in rats that inhaled 1-bromopropane vapor

Toru ISHIDAO[1], Yukiko FUETA[1], Susumu UENO[2], Yasuhiro YOSHIDA[3], and Hajime HORI[1]

[1] Department of Environmental Management, School of Health Sciences, University of Occupational and Environmental Health, Japan.

[2] Department of Occupational Toxicology, Institute of Industrial Ecological Sciences, University of Occupational and Environmental Health, Japan.

[3] Department of Immunology and Parasitology, School of Medicine, University of Occupational and Environmental Health, Japan.

Correspondence to: Toru Ishidao, Department of Environmental Management, School of Health Sciences, University of Occupational and Environmental Health, Japan. Iseigaoka 1-1, Yahatanishi-ku, Kitakyushu 807-8555, Japan

(*e-mail: ishidao@health.uoeh-u.ac.jp*)

Running title: **A cross-fostering analysis of bromine ion concentration**

The number of words in the abstract: **238**; text: **2087**, and the number of tables: **2**; figures: **3**

Field: ***Toxicology***

1

Abstract: Objective: Inhaled 1-bromopropane decomposes easily and releases bromine ion. However, the kinetics and transfer of bromine ion into the next generation have not been clarified. In this work, the kinetics of bromine ion transfer to the next generation was investigated by using cross-fostering analysis and a one-compartment model. **Methods:** Pregnant Wistar rats were exposed to 700 ppm of 1-bromopropane vapor for 6 h per day during gestation days (GDs) 1–20. After birth, cross-fostering was performed between mother exposure groups and mother control groups, and the pups were subdivided into the following four groups: exposure group, postnatal exposure group, gestation exposure group, and control group. Bromine ion concentrations in the brain were measured temporally. **Results:** Bromine ion concentrations in mother rats were lower than those in virgin rats, and the concentrations in fetuses were higher than those in mothers on GD20. In the postnatal period, the concentrations in the gestation exposure group decreased with time, and the biological half-life was 3.1 days. Conversely, bromine ion concentration in the postnatal exposure group increased until postnatal day 4 and then decreased. This tendency was also observed in the exposure group. A one-compartment model was applied to analyze the behavior of bromine ion concentration in the brain. By taking into account the increase of body weight and change in the bromine ion uptake rate in pups, the bromine ion concentrations in the brains of the rats could be estimated with acceptable precision.

Key words: 1-Bromopropane inhalation, Cross-fostering, Bromine ion concentration, One-compartment model, Animal experiment

1-Bromopropane (1-BP, CAS no. 106-94-5) is widely used as a substitute for chlorofluorocarbons, which destroy the ozone layer. The toxicity of 1-BP has been

reviewed[1], and the Japan Society for Occupational Health recommends an occupation exposure limit of 0.5 ppm[2]. Previously, we studied the effects of inhaled 1-BP vapor in male rats on the nervous[3-8] and immune systems[9, 10].

We also studied the effects of inhaled 1-BP vapor on metabolism in male rats and reported that 1-BP rapidly decomposes and releases bromine ion in the blood[11], indicating that bromine ion is a major index of 1-BP exposure. Recently, because of the health effects reported in female workers exposed to 1-BP[12-14], there is concern regarding the health effects of 1-BP exposure on the next generation. Some researchers have reported results of experiments in female animals[15-17]; however, the kinetics of bromine ion distribution to the next generation has not been elucidated. In this study, pregnant rats were exposed to 700 ppm of 1-BP vapor, and the concentration of bromine ion in the rat brain was measured. The distribution of bromine in fetuses and cross-fostered pups was investigated. A one-compartment model was employed to analyze the behavior of bromine ion in rats.

Methods

Animals

Female (9-week-old) and male (10-week-old) Wistar rats were purchased from Kyudo Co., Ltd. (Saga, Japan). After acclimation in polycarbonate cages with dry chips, they were housed in pairs in animal rooms under 12-h light–dark cycle conditions at 22 ± 1°C and 55 ± 5% relative humidity, with free access to food and water. The presence of sperm in the vaginal smear was defined as day 0 of gestation (GD0; female rats were 11 weeks old). In the inhalation study, the female rats were divided into three groups: 1-BP-exposed virgin female group (n = 5), 1-BP-exposed mother group (n = 11), and the control mother group (n = 5). After the final exposure of mother rats on GD20, they

were housed in an animal room for the onset of birth. Postnatal day (PND) i.e., the day after birth, was defined as day 0 (PND0 = GD21). On PND1, a litter size of eight pups was assembled and cross-fostering[17, 18] of pups was performed between mother exposure groups (n = 3) and mother control groups (n = 3). The pups were subdivided into four groups: (1) exposure group (1-BP-exposed pups were raised by their birth mother exposed to 1-BP), (2) postnatal exposure group (control pups were raised by 1-BP-exposed mother), (3) gestation exposure group (1-BP-exposed pups were raised by control mother), and (4) control group (control pups were raised by their control mother). The experimental groups are summarized in Table 1. Body weight was measured periodically. The experiments were conducted per the guidance of the Ethics Committee of Animal Care and Experimentation in accordance with The Guiding Principle for Animal Care Experimentation, University of Occupational and Environmental Health, Japan (AE03-065), which conforms to the National Institutes of Health Guide for the Care and Use of Laboratory Animals and the Japanese Law for Animal Welfare and Care.

Exposure

Reagent-grade 1-BP was obtained from Kanto Chemical Co., Ltd. (Tokyo, Japan). 1-BP vapor was introduced into a 400-*l* stainless-steel exposure chamber. Details of this apparatus and procedure have been given elsewhere[11]. In order to study change in bromine ion in blood and brain when the condition of dysfunction of feedback inhibition (i.e., disinhibition) was confirmed, exposure concentration was designed to be 700 ppm, which was higher than LOAEL (400 ppm) for disinhibition[7]. The actual concentration of 1-BP vapor in the chamber was 701.3 ± 5.2 ppm. In the control group, only clean air was introduced into the chamber. The exposure period was 6 h per day

between 9 a.m. and 3 p.m. throughout gestation or GD1-20 (virgin female group was exposed until GD21). Table 1 displays the age of the rats on sampling day. They were deeply anesthetized with diethyl ether and then decapitated. The brains and the stomachs with milk from only the exposure group on PND1 were gently removed and stored in a freezer.

Measurement of bromine ion concentration

The brains (cerebrum and diencephalon) and stomachs (0.25 g) were homogenized with water (1.5 m*l*) at 0°C. The sample (1 m*l*) was dispensed into a vial, and 0.1 m*l* of dimethyl sulfate was added to convert bromine ion to methyl bromide. Then, 0.1 m*l* of an aqueous solution of isopropyl alcohol (0.5 volume percent) was added as an internal standard. The vial was heated at 50°C for 1 h. The bromine ion concentration was determined by measuring peak area of methyl bromide vapor in the headspace by using a gas chromatograph mass spectrometer (GC/MS, QP-5050; Shimadzu, Kyoto, Japan)[11].

Estimation method of bromine ion concentration

As previously described, inhaled 1-BP was metabolized and bromine ions were released. In this study, the behavior of released bromine ion concentration in the brain was analyzed by using a one-compartment model[19]. We assumed the bromine ion uptake rate, i.e., the generation rate of bromine ion, is equal to the 1-BP uptake rate because 1-BP is decomposed quickly[11] and releases bromine ion. Under this assumption, mass balance equations of bromine ion during exposure and clearance periods respectively were as follows:

$$\frac{dx}{dt} = R - kx \tag{1}$$

$$\frac{dx}{dt} = -kx \tag{2}$$

where x is the amount of bromine ion (μg); t is time (h); R is the generation rate of bromine ion (μg/h), which corresponds to the 1-BP uptake rate; and k is the excretion rate constant (1/h). From equations (1) and (2), the bromine ion concentrations C (μg/g) during exposure and clearance respectively were obtained as follows:

$$C = \frac{R}{\rho V k}\left(1 - e^{-kt}\right) \tag{3}$$

$$C = C_0 e^{-kt} \tag{4}$$

where V is the volume of the compartment (ml), ρ is the density of the compartment (g/ml), and C_0 is the initial concentration during clearance (μg/g). The excretion rate constant k is given by the biological half-life, $t_{1/2}$ (h) or $T_{1/2}$ (days).

$$k = \frac{\ln 2}{t_{1/2}(\mathrm{h})} = \frac{0.693}{T_{1/2}(\mathrm{days}) \times 24} \tag{5}$$

Experimental Results

Fig. 1 shows the change in the average body weight of mother rats exposed to 700 ppm of 1-BP up to GD20 and that of the pups after the exposure. The time, T (on the

horizontal axis), includes the GDs and PNDs. Litter sizes of exposed mothers and control mothers were 15.0 ± 2.8 and 14.9 ± 2.5 pups, respectively. The body weight of both mothers and pups increased rapidly. This tendency was also observed in the control group, and there was no significant difference between the exposure group and the control group. For the virgin female group, body weight did not change significantly (271.1 ± 17.0 g) during GD1-20.

Bromine ion concentration in the rat brain (μg/g-brain) exposed to 700 ppm of 1-BP on GDs is presented as symbols in Fig. 2. The bromine ion concentration in mother rats was lower than that in virgin rats, and the concentration in fetuses was higher than that in mothers. Fig. 3 shows changes in bromine ion concentration in pup brain for PNDs. The concentration in the gestation exposure group decreased between PND4 and PND8, whereas that in the postnatal exposure group increased from PND2 to PND4 and then decreased. This tendency was also observed in the exposure group, although the concentration on PND1 was lower than that on GD20 (fetus in Fig. 2). Specifically, the concentration in the exposure group was the highest just after birth, but decreased at PND1. The concentration then increased from PND1 to PND3, but decreased again with time. In the control pups, the bromine ion concentration was 11.2 ± 7.7 μg/g-brain on PND3.

The bromine ion concentration in pup stomachs with milk from the exposure group on PND1 was 830.6 ± 188.8 μg/g-stomach, which was about twice as much as that in the mother brain at GD20 (Fig. 2).

Discussion

The one-compartment model was applied to analyze the bromine ion concentration in the brains of virgin females, mothers, fetuses, and pups. Equations (3) and (4) have

two parameters, the excretion rate constant k and the 1-BP uptake rate R. The excretion rate constant, k, can be easily calculated from equation (5) by using the biological half-life $T_{1/2}$ (days). In our previous work[11], $T_{1/2}$ for male rats was 4.7–15.0 days in blood and 5.0–7.5 days in urine. Therefore, $T_{1/2}$ = 7.0 days was used for mothers and virgin females in this study. $T_{1/2}$ in pups was 3.1 days, obtained by experimental data. Equation (4) was applied to the data from PND1 for the exposure group and from PND4 and PND8 for the gestation exposure group as shown in Fig. 3. $T_{1/2}$ = 3.1 days was also used for fetuses. The half-lives of between GD20 for fetuses and PND1 for the exposure group were excluded from the calculation because of the time lag due to birth.

As shown in Fig. 2, the bromine ion concentration in the brains of mothers was lower than that in the brains of virgin females. A reason for this might be that the bromine ion concentration was diluted because of increasing body weight. The average body weight of pups, w (g), was expressed using the following equation (Fig. 1):

$$w = 0.00028T^{3.31} \tag{6}$$

The average body weight of mothers, W (g), was calculated as the sum of that of virgin females (ρV = 271.1 g) and of pups, w, (interpolated value for GDs):

$$W = 271.1 + 27w \tag{7}$$

where 27 is the constant, which was determined to give the best fit for the experimental data as shown in Fig. 1.

For virgin females, the uptake rate, R, of 2853 μg/h was obtained to give the best fit

of equations (3) and (4) for the experimental data on GD21 in Fig. 2. Therefore, $R/\rho V$ = R/W = 2853/271.1 = 10.5 μg/(h·g) for virgin females, and $R/\rho V$ = 2853/(271.1 + 27w) for mother rats was used in equation (3). For fetuses, R (bromine ion uptake rate from mothers) was assumed to be proportional to body weight, and $R/\rho V$ = R/w = 22.0 μg/(h·g) was applied, which was obtained to give the best fit for the experimental data on GD20 in Fig. 2. On PNDs, suckling (exposure to bromine ion from milk) was assumed to occur at 2-h intervals. As shown in Fig. 3, the curve of bromine ion concentration in the brains of the postnatal exposure group is convex. In addition, on PND1, the concentration in pup stomachs with milk was high, and the level was higher than that in the mother brain, as calculated using the one-compartment model (486.2 μg/g-brain). Therefore, we assume that the uptake rate R of pups is high at first and then decreases. In this work, R in the postnatal exposure group can be expressed by the following equation:

$$R = 388e^{-0.126(t-32)} \tag{8}$$

where 32 is the initial suckling (h) and 388 and 0.126 are the constants determined experimentally. The bromine ion concentration in the exposure group was calculated as the sum of the concentrations in the gestation exposure and postnatal exposure groups. Conditions of the one-compartment model and the values of parameters obtained are listed in Table 2. Solid, broken, and dotted lines in Fig. 2 indicate calculated lines for fetuses, mothers, and virgin females, respectively. In Fig. 3, solid, broken, and dotted lines indicate calculated lines of exposure, postnatal exposure, and gestation exposure groups, respectively. The lines calculated using the proposed model could be estimated from the experimental data with acceptable precision as shown in both figures.

The calculated bromine ion uptake rates per weight, $R/\rho V$, for adults and fetuses were 10.5 and 22 μg/(h·g), respectively. This result suggests that the bromine ion easily transfers from mothers to fetuses, and the concentration in fetuses was higher than that in mothers. R in postnatal exposure group was expressed as an exponential function, and $R/\rho V$ of 55 μg/(h·g) was obtained at initial suckling time. This value was large compared to 22 μg/(h·g), the calculated value at GD20, before birth. This suggests that uptake rate of bromine ion via milk was higher than that via the placenta, and the bromine ion concentration in the exposure group could be explained as the sum of that in the gestation and postnatal exposure groups, which is shown in Fig. 3.

In summary, the results of this study suggest (1) the concentration of bromine ion in mother rats was lower than that in virgin female rats, (2) bromine ion easily transferred from mothers to fetuses and accumulated before birth, (3) bromine ion was concentrated more in milk than in the brains of the mothers, and (4) bromine ion uptake rate in pups was high immediately after birth.

Acknowledgments:

The authors thank Ms. Tomoko Tanaka, Kana Hayashi, Erika Ito, and Ai Kanemaru for technical help and Dr. Sumiyo Ishimatsu for her critical comments on our experiments.

References

1) Ichihara G. Neuro-reproductive toxicities of 1-bromopropane and 2-bromopropane. Int Arch Occup Environ Health 2005; 78; 79-96.

2) The Japan Society for Occupational Health. Recommendation of occupational exposure limits (2013-14). J Occup Health 2013; 55; 422-41.

3) Ohnishi A, Ishidao T, Kasai T, Arashidani K, Hori H. Neurotoxicity of 1-bromopropane in rats. J UOEH 1999; 21; 23-8.

4) Fueta Y, Ishidao T, Kasai T, Hori H, Arashidani K. Decreased paired-pulse inhibition in the dentate gyrus of the brain in rats exposed to 1-bromopropane vapor. J Occup Health 2000; 42; 149-51.

5) Fueta Y, Ishidao T, Arashidani K, Endo Y, Hori H. Hyperexcitability of the hippocampal CA1 and the dentate gyrus in rats subchronically exposed to a substitute for chlorofluorocarbons, 1-bromopropane vapor. J Occup Health 2002; 44; 156-65.

6) Fueta Y, Fukuda T, Ishidao T, Hori H. Electrophysiology and immunohistochemistry in the hippocampal CA1 and the dentate gyrus of rats chronically exposed to 1-bromopropane, a substitute for specific chlorofluorocarbons. Neuroscience 2004; 124; 593-603.

7) Fueta Y, Ishidao T, Ueno S, Yoshida Y, Kunugita N, Hori H. New approach to risk assessment of central neurotoxicity induced by 1-bromopropane using animal models. Neurotoxicology 2007; 28; 270-3.

8) Ueno S, Yoshida Y, Fueta Y, Ishidao T, Liu JQ, Kunugita N, Yanagihara N, Hori H. Changes in the function of the inhibitory neurotransmitter system in the rat brain following subchronic inhalation exposure to 1-bromopropane. Neurotoxicology 2007; 28; 415-20.

9) Yoshida Y, Liu JQ, Nakano Y, Ueno S, Fueta Y, Ishidao T, Kunugita N, Yamashita U, Hori H. 1-BP inhibits NF-kB activity and Bcl-xL expression in astrocytes in vitro and reduces Bcl-xL expression in the brains of rats in vivo. Neurotoxicology 2007; 28; 381-6.

10) Yoshida Y, Nakano Y, Ueno S, Liu JQ, Fueta Y, Ishidao T, Kunugita N, Yanagihara N, Sugiura T, Yamashita U, Hori H. Effects of 1-bromopropane, a substitute for chlorofluorocarbons, on brain-derived neurotrophic factor (BDNF) expression. Int Immunopharmacol 2009; 9; 433-8.

11) Ishidao T, Kunugita N, Fueta Y, Arashidani K, Hori H. Effects of inhaled 1-bromopropane vapor on rat metabolism. Toxicol Lett 2002; 134; 237-43.

12) Ichihara G, Miller JK, Ziolkowska A, Itohara S, Takeuchi Y. Neurological disorders in three workers exposed to 1-bromopropane. J Occup Health 2002; 44; 1-7.

13) Ichihara G, Li W, Ding X, Peng S, Yu X, Shibata E, Yamada T, Wang H, Itohara S, Kanno S, Sakai K, Ito H, Kanefusa K, Takeuchi Y. A survey on exposure level, health status, and biomarkers in workers exposed to 1-bromopropane. Am J Ind Med 2004; 45; 63-75.

14) Li W, Shibata E, Zhou Z, Ichihara S, Wang H, Wang Q, Li J, Zhang L, Wakai K, Takeuchi Y, Ding X, Ichihara G. Dose-dependent neurologic abnormalities in workers exposed to 1-bromopropane. J Occup Environ Med 2010; 52; 769-77.

15) Sekiguchi S, Suda M, Zhai YL, Honma T. Effects of 1-bromopropane, 2-bromopropane, and 1,2-dichloropropane on the estrous cycle and ovulation in F344 rats. Toxicol Lett 2002; 126; 41-9.

16) Yamada T, Ichihara G, Wang H, Yu X, Maeda K, Tsukamura H, Kamijima M, Nakajima T, Takeuchi Y. Exposure to 1-bromopropane causes ovarian dysfunction in rats. Toxicol Sci 2003; 71; 96-103.

17) Furuhashi K, Kitoh J, Tsukamura H, Maeda K, Wang H, Li W, Ichihara S, Nakajima T, Ichihara G. Effects of exposure of rat dams to 1-bromopropane during pregnancy and lactation on growth and sexual maturation of their offspring. Toxicology 2006; 224; 219-28.

18) Lau C, Thibodeaux JR, Hanson RG, Rogers JM, Grey BE, Stanton ME, Butenhoff JL, Stevenson LA. Exposure to perfluorooctane sulfonate during pregnancy in rat and mouse. II: postnatal evaluation. Toxicological Sci 2003; 74; 382-92.

19) Hori H, Hyakudo T, Oyabu T, Ishimatsu S, Yamato H, Tanaka I. Effects of inhaled methyl bromide gas on the metabolic system and kinetics of bromine ion in rats. J UOEH 2002; 24; 151-60.

Table 1. Experimental groups and ages of adult and fetal rats exposed to 700 ppm of 1-BP and of pups on sampling day

Groups (n)		Age (n) on sampling day
Virgin female	Exposure (5)	GD21 (2)
Mother	Exposure (11) Control (5)	GD20 (3)
Fetus	Exposure	GD20 (13)
Pup†	Exposure Postnatal exposure Gestation exposure Control	PND1 (10), PND3 (10), PND5 (5), PND7 (5) PND2 (5), PND4 (5), PND8 (5) PND4 (5), PND8 (5) PND3 (5)

1-BP: 1-bromopropane, GD: gestation day, PND: postnatal day, †: Exposure = 1-BP exposed pups were raised by their birth mother exposed to 1-BP, Postnatal exposure = control pups were raised by 1-BP exposed mother, Gestation exposure = 1-BP exposed pups were raised by control mother, Control = control pups were raised by control mother

Table 2. Parameters of the one-compartment model

Groups		$T_{1/2}$ (days)	ρV (g)	R (μg/h)	Results
GD	Virgin female	7.0	271.1	2853	Fig. 2
	Mother	7.0	271.1+27w	2853	Fig. 2
	Fetus	3.1	w	22w	Fig. 2
PND	Gestation exposure	3.1			Fig. 3
	Postnatal exposure	3.1	w	$388e^{-0.126(t-32)}$	Fig. 3
	Exposure	Gestation exposure + Postnatal exposure			Fig. 3
	Mother	7.0			Text†

†: the concentration in mother brain corresponding to PND1 (486.2 μg/g-brain),
$w=0.00028T^{3.31}$ by equation (6)

Figure Captions

Fig. 1. The average body weight of mothers (*W*) exposed to 700 ppm of 1-BP up to GD20 and that of pups (*w*) after exposure. 1-BP: 1-bromopropane; GD: gestation day; PND: postnatal day

Fig. 2. Change in bromine ion concentration in rat brain exposed to 700 ppm of 1-BP on GDs. Symbols represent experimental data: ●, fetus; ▲, mother; △, virgin female. Solid, broken, and dotted lines indicate calculated lines for fetuses, mothers, and virgin females, respectively. 1-BP: 1-bromopropane; GD: gestation day

Fig. 3. Change in bromine ion concentration in pup brain during PNDs. Symbols represent experimental data: ●, exposure group (1-BP exposed pups were raised by their birth mother exposed to 1-BP); ◇, postnatal group (control pups were raised by 1-BP exposed mother); □, gestation exposure (1-BP exposed pups were raised by control mother). Solid, broken, and dotted lines indicate calculated lines for exposure, postnatal exposure, and gestation exposure groups, respectively. 1-BP: 1-bromopropane; PND: postnatal day

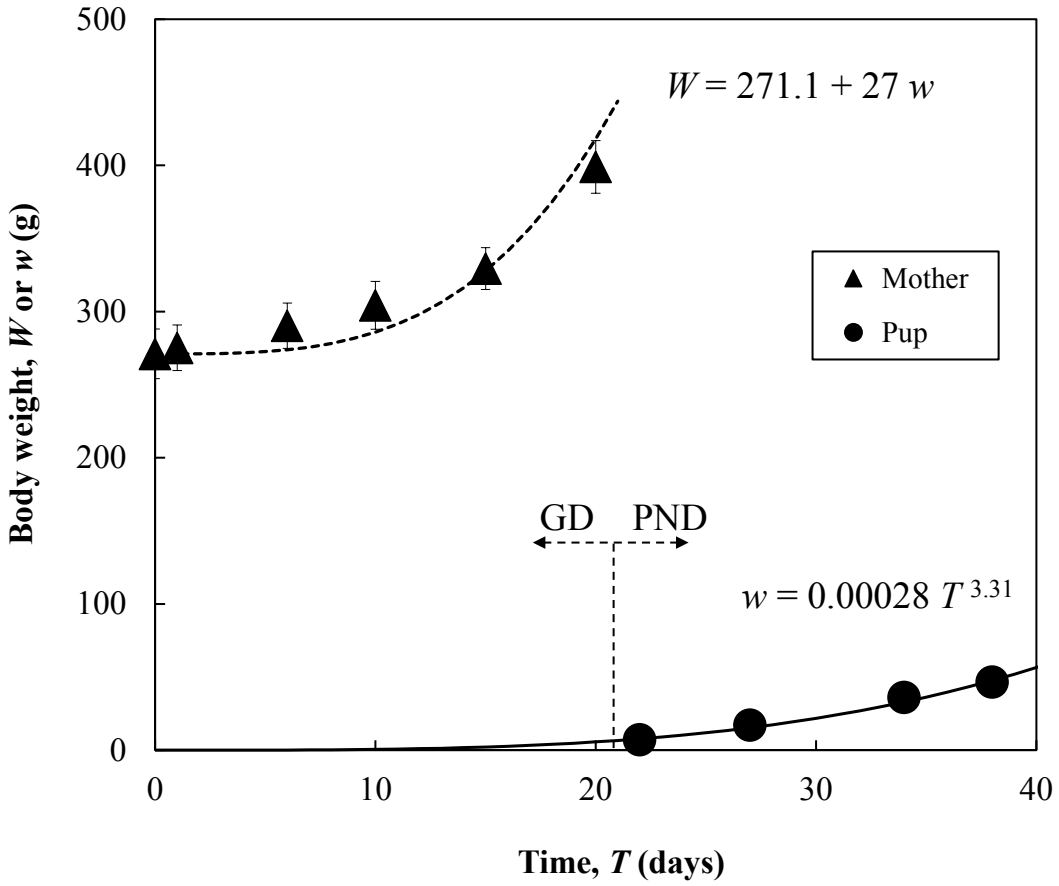
500
400
300
200
100
0
0
10
20
30
40
Body weight, W or w (g)
Time, T (days)
W = 271.1 + 27 w
Mother
Pup
GD
PND
w = 0.00028 T 3.31

Fig. 1.

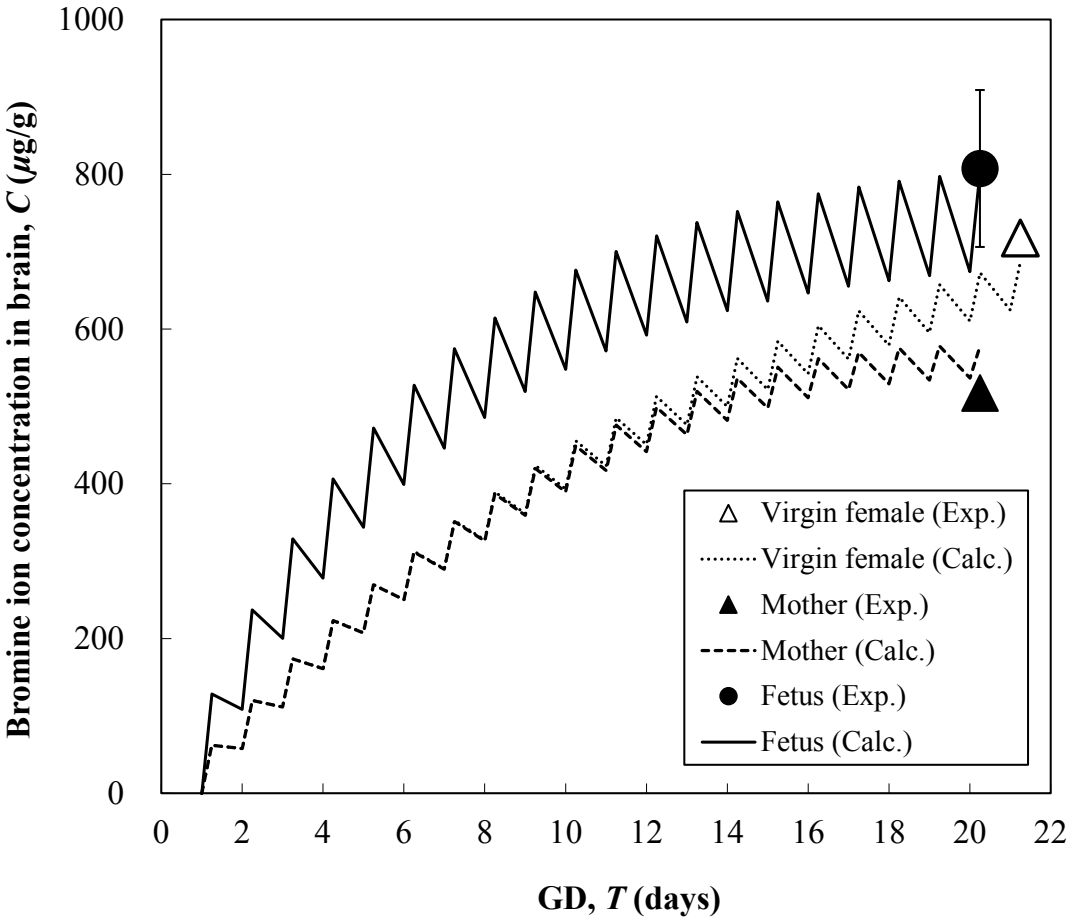
Bromine ion concentration in brain, C (μg/g)
1000
800
600
400
200
0
0
2
4
6
8
10
12
14
16
18
20
22
GD, T (days)
Virgin female (Exp.)
Virgin female (Calc.)
Mother (Exp.)
Mother (Calc.)
Fetus (Exp.)
Fetus (Calc.)

Fig. 2.

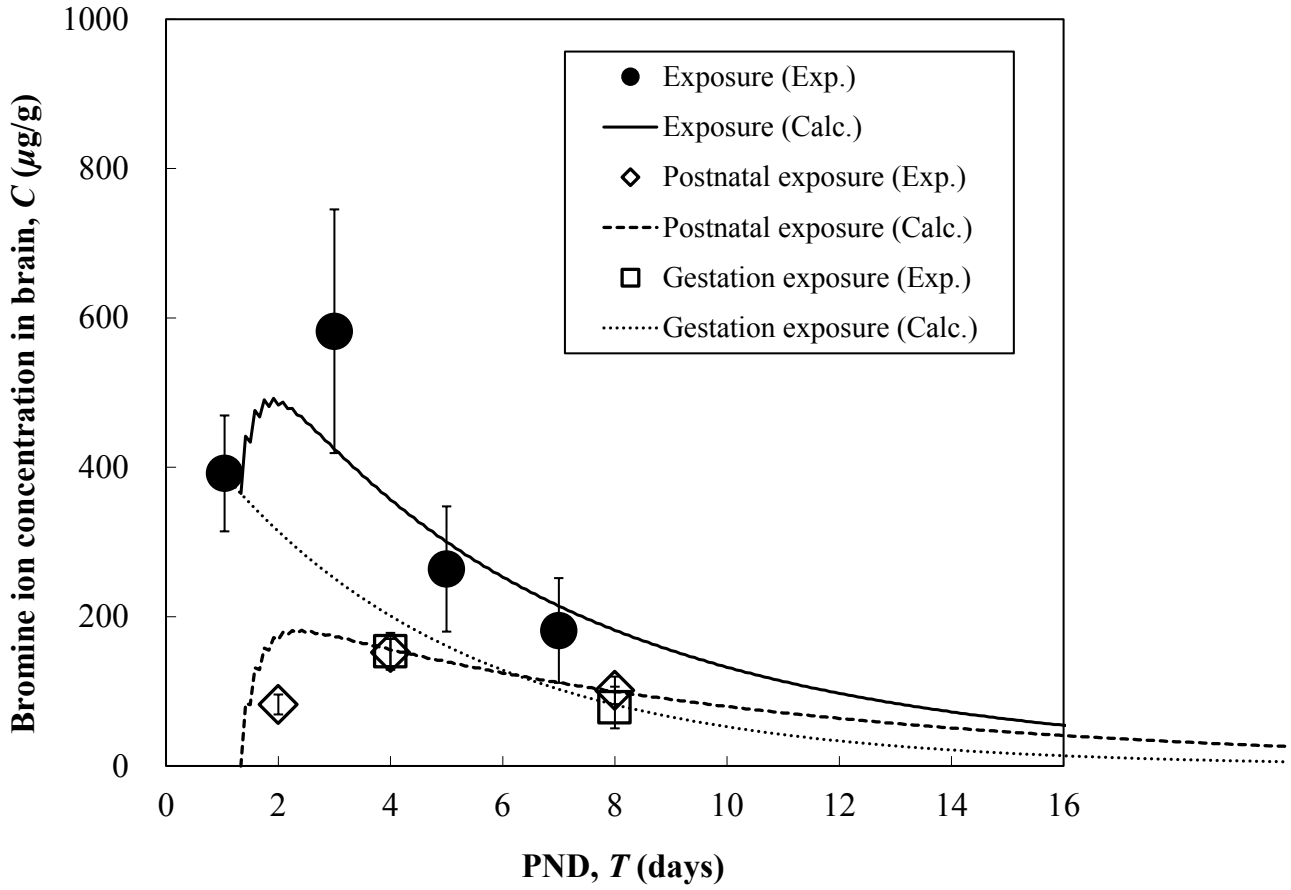
Bromine ion concentration in brain, C (μg/g)
1000
800
600
400
200
0
0
2
4
6
8
10
12
14
16
PND, T (days)
Exposure (Exp.)
Exposure (Calc.)
Postnatal exposure (Exp.)
Postnatal exposure (Calc.)
Gestation exposure (Exp.)
Gestation exposure (Calc.)

Fig. 3.

[Research Note]

Prenatal Exposure to 1-Bromopropane Suppresses Kainate-Induced Wet Dog Shakes in Immature Rats

Yukiko FUETA[1*], Masanari KANEMITSU[1], Sumie EGAWA[1], Toru ISHIDAO[1], Susumu UENO[2] and Hajime HORI[1]

[1] *Department of Environmental Management, School of Health Sciences, University of Occupational and Environmental Health, Japan. Yahatanishi-ku, Kitakyushu 807-8555, Japan*

[2] *Department of Occupational Toxicology, Institute of Industrial Ecological Sciences, University of Occupational and Environmental Health, Japan. Yahatanishi-ku, Kitakyushu 807-8555, Japan*

Abstract : 1-Bromopropane (1-BP) is used in degreasing solvents and spray adhesives. The adverse effects of 1-BP have been reported in human cases and adult animal models, and its developmental toxicity has also been reported, but its effects on developmental neurotoxicity have not been investigated in detail. We evaluated the effects in rat pups of prenatal exposure to 1-BP on behaviors such as scratching and wet dog shakes (WDS), which were induced by injection of kainate (KA). Pregnant Wistar rats were exposed to vaporized 1-BP with 700 ppm from gestation day 1 to day 20 (6 h/day). KA at doses of 0.1, 0.5, and 2.0 mg/kg were intraperitoneally injected into a control group and a 1-BP-exposed group of pups on postnatal day 14. There was no significant difference in scratching between the control and the prenatally 1-BP-exposed groups, while suppression of the occurrence ratio of WDS was observed at the low dose of 0.1 mg/kg of KA in the prenatally 1-BP-exposed pups. Our results suggest that prenatal exposure to 1-BP affects neurobehavioral responses in the juvenile period.

Keywords : 1-bromopropane, prenatal exposure, developmental neurotoxicity, wet dog shake, rats.

(Received June 26, 2015, accepted November 9, 2015)

Introduction

The volatile organic compound 1-bromopropane (CH_3-CH_2-CH_2Br; 1-BP), a substitute for specific chlorofluorocarbons, is mainly used in degreasing solvents and spray adhesives. It has been reported that occupational exposure to 1-BP causes neurotoxicity, such as numbness, gait disturbance, prolongation of distal latency and memory dysfunction [1].

Animal models exposed to 1-BP have also shown central neurotoxicity, including ataxic gait, prolongation of distal latency, alteration of mRNA levels of neurotransmitter receptors [1], and hippocampal disinhibition [2]. *In vitro* studies have revealed that the direct application of 1-BP enhanced the currents mediated by the activation of A type γ-aminobutyric acid ($GABA_A$) receptors, suppressed the currents mediated by neuronal nicotinic acetylcholine receptors, and potentiated feedback inhibition in the cornu ammonis 1 (CA1) subfield of hippocampal slices [3]. The gene expression of the B-cell lymphoma-extra large molecule (Bcl-xl), and the activity of nuclear factor-kappa B (NF-κB), were suppressed in *in vitro* and *in vivo* studies [4]. The developmental effects of 1-BP have also been investigated [5], but little is known about the developmental neurotoxicity in offspring.

*Corresponding Author: Yukiko FUETA, Department of Environmental Management, School of Health Sciences, University of Occupational and Environmental Health, Japan. Yahatanishi-ku, Kitakyushu 807-8555, Japan, Tel: +81-93-603-1611, Fax: +81-93-691-2694, E-mail: yukiko@med.uoeh-u.ac.jp

In our previous study of the developmental neurotoxicity of 1-BP, prenatal exposure to 1-BP altered hippocampal excitability and the gene expression of the Na^+ channel [6] and glutamate receptor subunits on postnatal day (PND) 14 [7]. These results raised the possibility that prenatal exposure to 1-BP affects brain development and its related behaviors. However, conventional behavioral tests for rodents are difficult to apply to pups. Thus, we focused on the particular behaviors of scratching and wet dog shakes (WDS), which can be observed in pups.

Scratching is defined as repetitive and quick flexion-extension movements of the hind limbs toward the neck or the head region. This behavior has been shown to be spontaneously induced in normal as well as pathological conditions and is used as an itch model in rodents [8], although the behavior in pups remains to be analyzed. WDS is characterized as brief and fierce shaking of the head, neck, and trunk, appearing when rodents are wet, as the name suggests [9]. Interestingly, it has been reported that both scratching and WDS can be induced by electrical stimulation of limbic structures [10], and by several pharmacological interventions, such as kainate (KA) [9, 11] and pentylenetetrazole. KA is the agonist of ionotropic glutamate receptors, which mediate excitatory neurotransmission and are predominantly distributed in the hippocampus, inner lamina of the neocortex, and ventral thalamus [12]. Thus, scratching and WDS induced by KA could be useful indices of changes in the excitatory neurotransmission of neuronal networks in pup brains. In this study, we examined the effect of prenatal exposure to 1-BP on behaviors in pups by evaluating the incidences of scratching and WDS induced by KA.

Materials and Methods

Animals and 1-BP inhalation

Thirty-two female and 16 male Wistar rats (designated the parental (P) generation) purchased from Kyudo *Co.* (Tosu, Japan) at 11 weeks of age were housed in plastic cages with paper-made chips (ALPHA-dri, Shepherd Specialty Papers, Milford, USA) on a 12 h light/dark cycle (light period: 07:00-19:00). The room temperature was kept at 23 ± 1°C. The relative humidity was about 70%. The animals had free access to food and water. Proestrus stage was verified with an impedance checker (MK-10B, Muromachi Kikai *Co., Ltd.*, Tokyo, Japan). When the impedance was over three kΩ, the F0 female rats were mated with male rats. In the morning of the following day, the existence of sperm in the vaginal smear or vaginal plug was verified as the gestation day (GD) 0. Fourteen dams from the colony were used in the experiment. The pregnant rats of the P generation were randomly divided into two groups (7 rats in each): one group as the control and the other for exposure to 1-BP.

1-BP was purchased from Kanto Chemical *Co., Ltd.* (Tokyo, Japan). Seven dams were exposed to 1-BP vapor at a concentration of 700 ppm (6 h/day) for 20 days from GDs 1 to 20 in an exposure chamber [13], whereas the other seven dams were provided fresh air in the same type of chamber. Both P generation groups were not allowed access to food and water during the inhalation period. Four weeks of 1-BP inhalation (700 ppm) resulted in apparent effects on the hippocampus in the adult rats [2]. Therefore, we first chose the concentration of 700 ppm to study the possible underlying mechanism of developmental neurotoxicity in prenatally 1-BP-exposed rats. The concentration of 1-BP was monitored with a gas chromatograph (GC353B FSL, GL Sciences *Inc.*, Japan) equipped with a flame ionization detector.

All the pregnant rats gave birth to offspring (termed the first filial (F1) generation) on GD 21. The day of birth was defined as PND 0. We randomly gathered 26 F1 rats from the 7 control litters and 22 F1 rats from the 7 1-BP-exposed litters. All the F1 pups were bred with their mother rats during the lactation period. In this study, 24 female and 3 male F1 rats were obtained from the 7 dams in the control group, and 18 female and 4 male F1 rats were obtained from the 7 dams in the 1-BP-exposed group, respectively. We examined the F1 rats for the general toxicity of 1-BP inhalation exposure, such as litter size, sex ratio, testicular descent, vaginal opening, ear opening, and survival rate. The body weight of the F1 rats was measured on PND 14.

KA administration and behavioral observation

KA was obtained from Wako Pure Chemical Industries, *Ltd.* (Osaka, Japan). KA (0.1, 0.5, and 2.0 mg/kg) was dissolved in phosphate buffered saline (PBS).

PBS or KA was intraperitoneally injected to the F1 rats at PND 14, after which the F1 rats were placed in a clear plastic cage, and the scratching and WDS were observed by video-recording for 180 min in a room for the behavioral observation. The room temperature was kept at about 25°C. The behavioral observation was conducted for 180 min between 09:30 and 15:30. The number of F1 rats that showed the scratching and the WDS behavior was counted and then the occurrence ratio was calculated. The duration and frequency of scratching and WDS were also measured. This experiment was approved by the Ethics Committee for Animal Care and Experimentation in accordance with the University of Occupational and Environmental Health, Japan.

All the chemicals used in this study were a reagent grade and purchased from commercial sources.

Statistical analysis

The difference in bodyweight between the F1 control and F1 1-BP-exposed groups was analyzed by Student *t*-test. The Mantel-Haeinzel procedure was utilized to see the whole effect of the prenatal inhalation of 1-BP on the occurrence ratio of scratching and WDS. When appropriate, Fisher's exact test determined significant differences. A two-way analysis of variance (ANOVA) was performed to clarify the effects of prenatal exposure to 1-BP and/or a dose of KA on the frequency and the duration of scratching and WDS. When appropriate, *post hoc* analysis by Scheffe's test determined significant differences, respectively. The criteria of significant difference was $P < 0.05$ in all the statistical analyses. Data represent mean ± standard error of the mean (SEM).

Results and Discussion

General toxicity of 1-BP inhalation exposure in F0 and F1 generations

There were no outward pathological signs related to 1-BP in the F0 rats. The body weights of the P generation dams treated with 1-BP were not significantly different from those in the control (fresh air) group (data not shown). None of the F1 rats died during the experimental period, indicating that the exposure seemed to cause little stress on the dams in this study. There was no difference in the sex ratio, survival rate, or other clinical signs between the F1 control and F1 1-BP-exposed groups, with the exception of body weight. The body weight in the female F1 1-BP-exposed group (32.5 ± 0.5 g) was significantly lower ($P < 0.01$, Student *t*-test) than that in the female F1 control group (35.0 ± 0.4 g). The 1-BP-exposed male F1 rats also had a lower body weight (33.5 ± 0.3 g) compared to the male F1 control group (37.0 ± 0.8 g) ($P < 0.01$, Student *t*-test). Our results were consistent with previous studies showing that prenatal exposure to 1-BP has no effects on postnatal survival rate, excluding the body weight [5].

Effect of prenatal exposure to 1-BP on behavioral responses

KA administration elicits immobilization, followed by scratching, WDS, forelimb clonus, and status epilepticus (continuous chronic-tonic posturing of all 4 limbs) [11]. It is also known that a low dose less than 3 mg/kg of KA elicits scratching and WDS but hardly ever elicits epileptic convulsions. Our preliminary study also showed that doses of KA higher than 4 mg/kg induced convulsive behaviors as well as scratching and WDS, thus we chose doses of 0.1, 0.5, and 2.0 mg/kg of KA.

Behavioral data obtained from both genders is combined in Tables 1 and 2, because it has been reported that there are no sex differences in KA induced-behaviors in pups [14].

In the F1 control group, all of the tested pups showed scratching during the 180 min after injection of PBS or KA. The frequency and duration of the scratching was significantly higher only at the dose of 2.0 mg/kg (Table 1). WDS were observed in 80% of the PBS-injected control pups and in all of the KA-injected control pups. A significantly higher frequency of WDS was observed at the dose of 2.0 mg/kg (Table 2). The behavioral changes induced by the KA doses of 0.1 and 0.5 mg/kg were similar to those of PBS, thus it can be said that these two doses are subclinical.

Spontaneous scratching and WDS were also observed in the F1 1-BP-exposed group. The occurrence ratio of scratching was 100% at all doses of KA (Table 1), whereas that of WDS was 40 to 60% in 0 to 0.5 mg/kg and 100% in 2.0 mg/kg of KA (Tables 2). The effect of prenatal exposure to 1-BP was observed

in the occurrence ratio of WDS ($P < 0.01$; Mantel-Haenszel test). The occurrence ratio in the F1 1-BP-exposed group at 0.1 mg/kg KA was lower than that in the F1 control group ($P < 0.05$ by Fisher's exact test). The dose of 0.5 mg/kg KA tended to decrease the occurrence ratio in the F1 1-BP-exposed group, but did not reach a significant level. Taken together with the results of the 0.1 and 0.5 mg/kg KA (subclinical doses), the occurrence ratio (6 out of 12 rat pups) in the F1 1-BP-exposed group exhibited a lower value than that in the F1 control group (16 out of 16 rat pups, $P < 0.005$ by Fisher's exact test). This indicates that the effects of prenatal 1-BP exposure can be observed only at the subclinical doses of KA. The duration and the frequency of the scratching and the WDS increased at the dose of 2.0 mg/kg ($P < 0.01$), but we did not find any significant effect of prenatal 1-BP exposure on the duration and frequency of WDS at any of the doses of KA. Our results suggest that prenatal exposure to 1-BP suppresses the occurrence of WDS only at a low dose of KA, possibly due to an effect on mechanisms underlying the generation of WDS.

WDS can be induced by electrical stimulation of limbic structures and by the administration of several chemicals, such as serotonergic compounds [15] and an opioid receptor agonist [16], as well as KA. KA-induced-WDS is depressed by μ-opioid receptor antagonists [16]. An antagonist of α-amino-3-hydroxy-5-methyl-4-isoxazolepropionic acid/KA receptors suppresses WDS induced by serotonin receptor agonists [15]. The mechanisms of WDS induction by these chemicals are assumed to be related to each other. Besides those receptors, nitric oxide has also been demonstrated to play a regulatory role in KA- and getting-wet-induced-WDS [9]. These receptors and nitric oxide might be the target of prenatal exposure to 1-BP.

Table 1. The occurrence ratio, duration and frequency of scratching in F1 control and 1-BP-exposed groups

	F1 control			F1 1-BP-exposed		
KA (mg/kg)	S/N	duration (s)	frequency (counts)	S/N	duration (s)	frequency (counts)
PBS	5/5	1.9 ± 0.3	21 ± 6	5/5	2.3 ± 0.3	17 ± 5
0.1	11/11	2.0 ± 0.1	14 ± 2	7/7	2.0 ± 0.1	26 ± 10
0.5	5/5	1.7 ± 0.3	25 ± 4	5/5	2.1 ± 0.5	20 ± 8
2.0	5/5	2.9* ± 0.4	557* ± 164	5/5	3.6* ± 0.2	517* ± 41

F1: first filial generation, 1-BP: 1-bromopropane, KA: kainate, PBS: phosphate buffered saline, S: the number of rats in which scratching was observed, N: the total number of rats used in the experiment, S/N: the occurrence ratio, *: significant effects of KA on the duration or the frequency by two-way ANOVA followed by Scheffe's test ($P < 0.01$), mean ± SEM: mean ± standard error of the mean

Table 2. The occurrence ratio, duration and frequency of WDS in F1 control and 1-BP-exposed groups

	F1 control			F1 1-BP-exposed		
KA (mg/kg)	S/N	duration (s)	frequency (counts)	S/N	duration (s)	frequency (counts)
PBS	4/5	0.3 ± 0.02	1.8 ± 0.6	3/5	0.2 ± 0.03	0.8 ± 0.4
0.1	11/11	0.3 ± 0.03	3.4 ± 0.6	4/7[a]	0.3 ± 0.09	1.0 ± 0.4
0.5	5/5	0.3 ± 0.02	2.6 ± 0.9	2/5	0.2, 0.3	0.8 ± 0.6
2.0	5/5	0.3 ± 0.05	29.2* ± 10.0	5/5	0.4 ± 0.02	54.4* ± 21.1

WDS: wet dog shakes, F1: first filial generation, 1-BP: 1-bromopropane, KA: kainate, PBS: phosphate buffered saline, S: the number of rats in which WDS were observed, N: the total number of rats used in the experiment, S/N: the occurrence ratio, a: a significant difference between F1 control and F1 1-BP-exposed groups at the dose of 0.1 mg/kg in the Fisher's exact test ($P < 0.05$), *: significant effects of KA ($P < 0.01$) on the two-way ANOVA followed by Scheffe's test, mean ± SEM: mean ± standard error of the mean. The data of durations in the F1 1-BP-exposed group administered 0.5 mg/kg of KA are shown in the duration(s) column

There are studies suggesting that the hippocampus is the target of KA. KA receptors have been found in the hippocampus in rat pups [12], and epileptic discharges have been observed when KA-induced seizures occur [17]. Moreover, KA-induced WDS was accompanied by robust electrographic seizures recorded from the hippocampus [18]. On the other hand, Fueta *et al.* have reported that prenatal 1-BP exposure decreases the paired-pulse ratio of population spikes in the CA1 subfield of the dorsal hippocampus in PND14 rats [19]. A decrease in the paired-pulse ratio of the population spike is generally interpreted as an increase in an inhibition [2]. Thus, prenatal 1-BP exposure may disturb the propagation of hyperactivity in the hippocampus, such as electrographic discharges associated with KA-induced WDS. This may account for the suppression of WDS by prenatal exposure to 1-BP. However, it should also be considered that the dentate gyrus (DG) in the ventral hippocampus is thought to be necessary for chemical interventions such as KA-, μ-opioid-, and electrical stimulation-induced WDSs in adult rats [16, 20, 21]. Therefore, further studies are needed to investigate the excitability of the DG in the ventral hippocampus in prenatally 1-BP-exposed rats.

In conclusion, we demonstrate here that prenatal exposure to 1-BP suppresses WDS induced by the administration of a low dose of KA. Our results indicate that prenatal 1-BP exposure may disturb the susceptibility to KA or the functions of neural networks related to the WDS. We also show that it may be advantageous to use pharmacological interventions with convulsants in investigations of the effects of environmental chemicals on behavioral responses in immature rats.

Conflict of Interest

No conflicts of interest to declare.

Acknowledgments

We gratefully acknowledge the animal care of K. Egashira. This study was partly supported by the Grants-in-Aid program of Japan Society for the Promotion of Science (No. 20591237, No. 23510084, and No.18510064), and a University of Occupational and Environmental Health (UOEH) Research Grant for Promotion of Occupational Health.

References

1. Ichihara G, Kitoh J, Li W, Ding X, Ichihara S & Takeuchi Y (2012): Neurotoxicity of 1-bromopropane: Evidence from animal experiments and human studies. J Adv Res 3: 91–98
2. Fueta Y, Ishidao T, Ueno S, Yoshida Y, Kunugita N & Hori H (2007): New approach to risk assessment of central neurotoxicity induced by 1-bromopropane using animal models. Neurotoxicology 28: 270–273
3. Ueno S, Fueta Y, Ishidao T, Yoshida Y, Tsutsui M, Toyohira Y, Hori H & Yanagihara N (2006): The central neurotoxicity of 1-bromopropane (1-BP), a substitute for chlorofluorocarbons: Studies on the effects caused by direct and subchronic exposure to 1-BP on hippocampal function. J Pharmacol Sci 100 (Suppl 1): 140
4. Yoshida Y, Liu JQ, Nakano Y, Ueno S, Ohmori S, Fueta Y, Ishidao T, Kunugita N, Yamashita U & Hori H (2007): 1-BP inhibits NF-κB activity and Bcl-xL expression in astrocytes in vitro and reduces Bcl-xL expression in the brains of rats *in vivo*. Neurotoxicology 28: 381–386
5. Huntingdon Life Sciences (2001): A developmental toxicity study in rat via whole body inhalation exposure. Study Number 98-4141. Ducument ID Title OAR-2002-0064: Document available in public dockets A-2001-07, OAR-2002-0064, and A-91-42. US EPA, Washington, DC
6. Ueno S, Fueta Y, Ishidao T, Yuhi T,Yoshida Y, Hori H & Yanagihara N (2008): Changes in the excitability and Na^+ channel gene expression in the hippocampus of postnatal 14 days-aged rats prenatally exposed to 1-bromopropane. Neurosci Res 61(1 Suppl): S269
7. Fueta Y, Ueno S, Ishidao T, Yoshida Y & Hori H (2009): Effects of prenatally exposed to 1-bromopropane on the brain of the young offspring. Neurosci Res 65 (Suppl 1): S250
8. Nojima H & Carstens E (2003): Quantitative assessment of directed hind limb scratching behavior as a rodent itch model. J Neurosci Methods 126: 137–143
9. Koylu EO, Uz T, Manev H & Pogun S (2002): Nitric oxide synthase inhibition suppresses wet dog shakes and augments convulsions in rats. Int J Neurosci 112: 291–300

10. Frush DP & McNamara JO (1986): Evidence implicating dentate granule cells in wet dog shakes produced by kindling stimulations of entorhinal cortex. Exp Neurol 92: 102–113
11. Albala BJ, Moshé SL & Okada R (1984): Kainic-acid-induced seizures: a developmental study. Brain Res 315: 139–148
12. Miller LP, Johnson AE, Gelhard RE & Insel TR (1990): The ontogeny of excitatory amino acid receptors in the rat forebrain–II. Kainic acid receptors. Neuroscience 35: 45–51
13. Ishidao T, Kunugita N, Fueta Y, Arashidani K & Hori H (2002): Effects of inhaled 1-bromopropane vapor on rat metabolism. Toxicol Lett 134 (1–3): 237–243
14. Doucette TA, Strain SM, Allen GV, Ryan CL & Tasker RA (2000): Comparative behavioral toxicity of domoic acid and kainic acid in neonatal rats. Neurotoxicol Teratol 22: 863–869
15. Gorzalka BB, Hill MN & Sun JC (2005): Functional role of the endocannabinoid system and AMPA/kainate receptors in 5-HT2A receptor-mediated wet dog shakes. Eur J Pharmacol 516: 28–33
16. Hong JS, Grimes L, Kanamatsu T & McGinty JF (1987): Kainic acid as a tool to study the regulation and function of opioid peptides in the hippocampus. Toxicology 46: 141–157
17. Ben-Ari Y, Tremblay E, Berger M & Nitecka L (1984): Kainic acid seizure syndrome and binding sites in developing rats. Brain Res 316: 284–288
18. Cherubini E, De Feo MR, Mecarelli O & Ricci GF (1983): Behavioral and electrographic patterns induced by systemic administration of kainic acid in developing rats. Brain Res 285: 69–77
19. Fueta Y, Ueno S, Ishidao T & Hori H (2010): Long-lasting effects on hippocampal excitability of the offspring prenatally exposed to 1-bromopropane, a substitute for specific chlorofluorocarbons. Neurosci Res 68 (Suppl 1): e417
20. Grimes LM, Earnhardt TS, Mitchell CL, Tilson HA & Hong JS (1990): Granule cells in the ventral, but not dorsal, dentate gyrus are essential for kainic acid-induced wet dog shakes. Brain Res 514: 167–170
21. Barnes MI & Mitchell CL (1990): Differential effects of colchicine lesions of dentate granule cells on wet dog shakes and seizures elicited by direct hippocampal stimulation. Physiol Behav 48: 131–138

1-ブロモプロパンへの胎生期曝露は発達期ラットにおいてカイニン酸で誘導されるWet Dog Shakesを抑制する

笛田　由紀子[1]，金光　雅成[1]，江川　純恵[1]，石田尾　徹[1]，上野　晋[2]，保利　一[1]

[1]産業医科大学　産業保健学部　作業環境計測制御学
[2]産業医科大学　産業生態科学研究所　職業性中毒学

要　　旨：1-ブロモプロパン(1-BP)は洗浄やスプレー接着剤の溶剤として用いられている．1-BPの有害性はヒトの事例や成獣を用いた動物で報告されてきた．発達毒性も報告されてはいるが，発達神経毒性についての詳細はわかっていない．我々は，1-BPの胎生期曝露が，発達期ラットへのカイニン酸投与により誘導される行動，すなわちscratching行動やwet dog shake様行動に及ぼす影響を調べた．ウィスター系妊娠ラットの妊娠1日目から20日目まで(6時間/日)，濃度700 ppmの1-BP蒸気を曝露した．生後14日目の対照群と1-BP曝露群にカイニン酸を0.1, 0.5, 2.0 mg/kgで腹腔内投与した．Scratching行動に関しては対照群と1-BP曝露群に違いは見られなかったが，wet dog shake様行動に関しては，低濃度である0.1 mg/kgにおいて発生率の低下が1-BP曝露群で見られた．1-BP胎生期曝露が発達期の神経行動に影響することが示唆された．

キーワード：1-ブロモプロパン，胎生期曝露，発達神経毒性，wet dog shake，ラット．

J UOEH(産業医大誌) 37(4)：255 − 261 (2015)

Naunyn-Schmiedeberg's Arch Pharmacol (2015) 388:1259–1269
DOI 10.1007/s00210-015-1161-y

ORIGINAL ARTICLE

Ikarisoside A inhibits acetylcholine-induced catecholamine secretion and synthesis by suppressing nicotinic acetylcholine receptor-ion channels in cultured bovine adrenal medullary cells

Xiaojia Li[1] · Yumiko Toyohira[1] · Takafumi Horisita[2] · Noriaki Satoh[3] · Keita Takahashi[1] · Han Zhang[4] · Munekazu Iinuma[5] · Yukari Yoshinaga[1] · Susumu Ueno[6] · Masato Tsutsui[7] · Takeyoshi Sata[2] · Nobuyuki Yanagihara[1]

Received: 20 April 2015 / Accepted: 27 July 2015 / Published online: 11 August 2015

Abstract Ikarisoside A is a natural flavonol glycoside derived from plants of the genus *Epimedium*, which have been used in Traditional Chinese Medicine as tonics, antirheumatics, and aphrodisiacs. Here, we report the effects of ikarisoside A and three other flavonol glycosides on catecholamine secretion and synthesis in cultured bovine adrenal medullary cells. We found that ikarisoside A (1–100 μM), but not icariin, epimedin C, or epimedoside A, concentration-dependently inhibited the secretion of catecholamines induced by acetylcholine, a physiological secretagogue and agonist of nicotinic acetylcholine receptors. Ikarisoside A had little effect on catecholamine secretion induced by veratridine and 56 mM K^+. Ikarisoside A (1–100 μM) also inhibited $^{22}Na^+$ influx and $^{45}Ca^{2+}$ influx induced by acetylcholine in a concentration-dependent manner similar to that of catecholamine secretion. In *Xenopus* oocytes expressing α3β4 nicotinic acetylcholine receptors, ikarisoside A (0.1–100 μM) directly inhibited the current evoked by acetylcholine. It also suppressed ^{14}C-catecholamine synthesis and tyrosine hydroxylase activity induced by acetylcholine at 1–100 μM and 10–100 μM, respectively. The present findings suggest that ikarisoside A inhibits acetylcholine-induced catecholamine secretion and synthesis by suppression of nicotinic acetylcholine receptor-ion channels in bovine adrenal medullary cells.

Keywords Adrenal medulla · Catecholamine secretion · *Epimedium* · Flavonoids · Ikarisoside A · Nicotinic acetylcholine receptor

✉ Nobuyuki Yanagihara
yanagin@med.uoeh-u.ac.jp

[1] Department of Pharmacology, University of Occupational and Environmental Health, School of Medicine, 1-1, Iseigaoka, Yahatanishi-ku, Kitakyushu 807-8555, Japan

[2] Department of Anesthesiology, University of Occupational and Environmental Health, School of Medicine, Yahatanishi-ku, Kitakyushu, Japan

[3] Shared-Use Research Center, University of Occupational and Environmental Health, Yahatanishi-ku, Kitakyushu, Japan

[4] Research Center of Traditional Chinese Medicine, Tianjin University of Traditional Chinese Medicine, Tianjin, China

[5] Department of Pharmacognosy, Gifu Pharmaceutical University, Daigakunishi, Gifu, Japan

[6] Department of Occupational Toxicology, Institute of Industrial Ecological Sciences, University of Occupational and Environmental Health, Yahatanishi-ku, Kitakyushu, Japan

[7] Department of Pharmacology, Faculty of Medicine, University of The Ryukyus, Nishihara, Okinawa, Japan

Introduction

Flavonoids, a group of secondary metabolites with variable phenolic structure, which exist widely in plants (Nijveldt et al. 2001; Ren and Zuo 2012), may exert potential benefits associated with reduced risks of age- and life style-related diseases such as cardiovascular diseases, diabetes, and some cancers (Lu et al. 2013; Yanagihara et al. 2014). Ikarisoside A is one of the flavonol derivatives derived from plants of the genus *Epimedium*, which have been used in Traditional Chinese Medicine as tonics, antirheumatics, and aphrodisiacs (Dou et al. 2006). Previous studies reported that the total flavonoid fraction of *Epimedium* extract suppresses urinary calcium excretion and improves bone properties in ovariectomized mice (Chen et al. 2011), and that other extracts with structures similar to that of ikarisoside A, such as icariin, can stimulate osteogenic activities (Zhou et al. 2013) and have

anti-inflammatory effects (Lai et al. 2013). Furthermore, ikarisoside A also has pharmacological effects such as antioxidant and anti-inflammatory effects (Choi et al. 2008) as well as anti-osteoporosis effects (Choi et al. 2010).

In the human body, the most abundant catecholamines are adrenaline, noradrenaline, and dopamine, all of which are produced from phenylalanine and/or tyrosine. Catecholamines are produced mainly in the chromaffin cells of the adrenal medulla, the postganglionic fibers of the sympathetic nervous system, and the central nervous system. Catecholamines play very important roles in heart rate, blood pressure, blood glucose levels, and the general reactions of the sympathetic nervous system.

Adrenal medullary cells derived from embryonic neural crests are functionally homologous to sympathetic postganglionic neurons. In bovine adrenal medullary cells, catecholamine secretion is associated with the activation of three types of ionic channels: nicotinic acetylcholine receptor (nAChR)-ion channels, voltage-dependent Na^+ channels, and voltage-dependent Ca^{2+} channels (Wada et al. 1985b). ACh induces Na^+ influx via nAChR-ion channels, then, it induces Ca^{2+} influx and subsequent catecholamine secretion (Wada et al. 1985b). On the other hand, stimulation of catecholamine synthesis induced by ACh is associated with the activation of tyrosine hydroxylase in cultured bovine adrenal medullary cells (Yanagihara et al. 1987; Tsutsui et al. 1994). The conversion of tyrosine to L-3,4-dihydroxyphenylalanine (DOPA) is the rate-limiting step of catecholamine biosynthesis (Nagatsu et al. 1964). Adrenal medullary cells have provided a good model for the detailed analysis of a drug's actions on catecholamine secretion and synthesis (Kajiwara et al. 2002; Toyohira et al. 2005; Shinohara et al. 2007).

In our previous study, we isolated 20 flavonol glycosides from *Epimedium* species, including ikarisoside A, icariin, epimedoside A, and epimedin C (Mizuno et al. 1988). Ikarisoside A showed neurite outgrowth activity in cultured PC12h cells (Kuroda et al. 2000). There is, however, little evidence regarding ikarisoside A's effects on sympathetic nervous system activity. In the present study, we investigated the effects of four flavonol glycosides on bovine adrenal medullary cell functions and found that ikarisoside A, but not the other three flavonol glycosides, inhibited ACh-induced catecholamine secretion and synthesis by suppression of nAChR-ion channels in the cells.

Materials and methods

Materials

Oxygenated Krebs-Ringer phosphate (KRP) buffer was used throughout unless stated otherwise. Its composition is as follows (in mM): 154 NaCl, 5.6 KCl, 1.1 $MgSO_4$, 2.2 $CaCl_2$, 0.85 NaH_2PO_4, 2.15 Na_2HPO_4, and 10 glucose, adjusted to pH 7.4. Drugs and reagents were obtained from the following sources: Eagle's minimum essential medium (Eagle's MEM) (Nissui Pharmaceutical, Tokyo, Japan); collagenase (Nitta Zerachin, Osaka, Japan); calf serum (Cell Culture Technologies, Gravesano, Switzerland). ACh and veratridine were from Sigma (St. Louis, MO, USA). L-[U-^{14}C]tyrosine was from American Radiolabeled Chemicals Inc. (St. Louis, MO, USA); $^{45}CaCl_2$, $^{22}NaCl$, and L-[1-^{14}C]tyrosine from Perkin-Elmer Life Sciences (Boston, MA, USA).

Isolation of flavonol glycosides from the leaves of *Epimedium* species

The leaves of *Epimedium diphyllum* were collected at Miyazaki Prefecture, Japan. Ikarisoside A and other flavonol glycosides were purified by high performance liquid chromatography, as reported previously (Mizuno et al. 1988). Ikarisoside A and other flavonol glycosides were dissolved in 100 % dimethyl sulfoxide (DMSO) and then diluted in a reaction medium before use at a final DMSO concentration not exceeding 0.5 %, unless otherwise specified. DMSO (0.5 %) did not influence the basal and ACh-induced catecholamine secretion in the present study (data not shown).

Primary culture of bovine adrenal medullary cells

Bovine adrenal medullary cells were isolated by collagenase digestion of adrenal medullary slices according to the method as reported previously (Yanagihara et al. 1979, 1996). Cells were suspended in Eagle's MEM containing 10 % calf serum, 3 μM cytosine arabinoside, and several antibiotics, and maintained in monolayer culture at a density of 4×10^6 cells/dish (35 mm dish; Falcon, Becton Dickinson Labware, Franklin Lakes, NJ, USA) or 10^6 cells/well (24-well plate; Corning Life Sciences, Lowell, MA, USA) at 37 °C under a humidified atmosphere of 5 % CO_2 and 95 % air. The cells were used for experiments between 2 and 5 days of culture.

Catecholamine secretion from cultured bovine adrenal medullary cells

The secretion of catecholamines was measured as described previously (Yanagihara et al. 1979). Cells (10^6/well) were washed three times with oxygenated KRP buffer, then firstly preincubated with or without ikarisoside A (0.3–100 μM) or other flavonol glycosides (10 μM) at 37 °C for 10 min, and incubated with or without ikarisoside A (0.3–100 μM) or other flavonol glycosides (10 μM) in the presence or absence of various secretagogues (300 μM ACh, 100 μM veratridine or 56 mM K^+) at 37 °C for another 10 min. After the reaction, the incubation medium was transferred immediately to a test tube containing perchloric acid (final concentration, 0.4 M) for the

full stop of the reaction. Catecholamines (noradrenaline and adrenaline) secreted into the medium were adsorbed onto aluminum hydroxide and estimated by the ethylenediamine condensation method (Weil-Malherbe and Bone 1952) using a fluorescence spectrophotometer (F-2500; Hitachi, Tokyo, Japan) with excitation and emission wavelengths of 420 and 540 nm, respectively.

$^{22}Na^{+}$ and $^{45}Ca^{2+}$ influx

The influx of $^{22}Na^{+}$ and $^{45}Ca^{2+}$ was measured as reported previously (Wada et al. 1985a, b). After preincubation with or without ikarisoside A (0.3–100 μM) at 37 °C for 10 min, cells (4×10^6/dish) were incubated with 1.5 μCi of $^{22}NaCl$ or 1.5 μCi of $^{45}CaCl_2$ at 37 °C for 5 min with or without 300 μM ACh and ikarisoside A (0.3–100 μM) in KRP buffer. After incubation, the cells were washed three times with ice-cold KRP buffer, solubilized in 10 % Triton X-100, and counted for radioactivity of $^{22}Na^{+}$ and $^{45}Ca^{2+}$ by a gamma counter (ARC-2005, Aloka, Tokyo, Japan) and a liquid scintillation counter (TRI-CARB 2900TR, PACKARD INSTRUMENT CO., Meriden, CT, USA), respectively.

^{14}C-Catecholamine synthesis from [^{14}C]tyrosine in the cells

After preincubation for 10 min, cells (4×10^6/dish) were incubated with 20 μM L-[U-^{14}C]tyrosine (1.0 μCi) KRP buffer in the presence or absence of various concentrations of ikarisoside A (0.3–100 μM) and 300 μM ACh at 37 °C for 20 min. After removing the incubation medium by aspiration, cells were harvested in 0.4 M perchloric acid and centrifuged at 1600×*g* for 10 min. ^{14}C-Catecholamines were separated further by ion exchange chromatography on Duolite C-25 columns (H^{+}-type, 0.4 × 7.0 cm) (Yanagihara et al. 1987) and counted for the radioactivity by a liquid scintillation counter (TRI-CARB 2900TR, PACKARD INSTRUMENT CO., Meriden, CT, USA). ^{14}C-Catecholamine synthesis was expressed as the sum of the ^{14}C-catecholamines (adrenaline, noradrenaline, and dopamine).

Tyrosine hydroxylase activity in situ

After preincubation with or without ikarisoside A (0.3–100 μM) for 10 min, cells (10^6/well) were exposed to 200 μl of KRP buffer with or without ikarisoside A (0.3–100 μM) and 300 μM ACh, supplemented with 18 μM L-[1-^{14}C]tyrosine (0.2 μCi) for 10 min at 37 °C. Upon addition of the labeled tyrosine, each well was sealed immediately with an acrylic tube capped with a rubber stopper and fitted with a small plastic cup containing 200 μl of NCS-II tissue solubilizer (GE Healthcare UK Ltd. Little Chalfont, Buckinghamshire, UK) to absorb the $^{14}CO_2$ released by the cells and counted for the radioactivity (Bobrovskaya et al. 1998).

Expression of α3β4 nAChRs in *Xenopus* oocytes and electrophysiological recordings

The complementary DNAs (cDNAs) encoding the α3 and β4 subunits of rat neuronal nAChR, subcloned into pcDNAI/Neo (Invitrogen, Carlsbad, CA) vector, were kindly provided from Dr. James W. Patrick (Division of Neuroscience, Baylor College of Medicine, TX, USA). After linearization of cDNA with *Not*I, complementary RNAs (cRNAs) were transcribed using T7 RNA polymerase from the mMESSAGE mMACHINE kit (Ambion, Austin, TX, USA). Adult female *Xenopus laevis* frogs were obtained from Kyudo Co., Ltd. (Saga, Japan). *Xenopus* oocytes and cRNA microinjection were prepared as described previously (Ueno et al. 2004; Horishita and Harris 2008). cRNAs of α3 and β4 subunits were co-injected at a same ratio (10–20 ng/50 nL) into *Xenopus* oocytes, and electrophysiological recordings were performed 2–6 days after injection. Oocytes were placed in a 100 μl recording chamber and perfused at 2 ml/min with extracellular Ringer solution (110 mM NaCl, 2.5 mM KCl, 10 mM HEPES, 1.8 mM $BaCl_2$, pH 7.5) containing 1.0 μM atropine sulfate. Ca^{2+} in the solution was replaced with Ba^{2+} to minimize the effects of secondarily activated Ca^{2+}-dependent Cl^{-} channels. Recording electrodes (1–3 MΩ) were filled with 3 M KCl, and the whole-cell voltage clamp was achieved through these two electrodes using a Warner Instruments model OC-725C (Warner, Hamden, CT, USA) at −70 mV. We measured the peak of the transient inward current in response to ACh that was applied for 30 s and examined the effects of ikarisoside A on a concentration of ACh that produced 50 % of the maximal effect (EC_{50}) of ACh. The EC_{50} was determined for each oocyte by 1 mM ACh that produces a maximal current. Ikarisoside A stocks were prepared in 100 % DMSO and diluted in bath solution to a final DMSO concentration not exceeding 0.1 %. Ikarisoside A was preapplied for 2 min to allow an equilibration with its site of interaction before ACh was added and its effect on the cation currents was determined. In all cases, between two currents, there was 10 min interval under washing with normal Ringer solution.

Statistical analysis

All experiments were performed in duplicate or triplicate, and each experiment was repeated at least three times. All values are given as means ± SEM. The significance of differences between means was evaluated using one-way analysis of variance (ANOVA). When a significant *F* value was found by ANOVA, Dunnett's or Scheffe's test for multiple comparisons was used to identify differences among the groups. Values were considered statistically different when *P* was less than

0.05. Statistical analyses were performed using PRISM for Windows version 5.0J software (Abacus Concept, Berkeley, CA, USA).

Results

The structures of four flavonol glycosides isolated from *Epimedium*

The four flavonol glycosides ikarisoside A, icariin, epimedin C, and epimedoside A were isolated from the leaves of *E. diphyllum* as reported previously (Mizuno et al. 1988). The structures of these four flavonol glycosides are shown in Fig. 1.

Effects of the flavonol glycosides on catecholamine secretion induced by various secretagogues in adrenal medullary cells

None of the four flavonol glycosides (ikarisoside A, icariin, epimedin C, and epimedoside A) at 10 μM significantly affected the basal secretion of catecholamines (Fig. 2a). ACh (300 μM), an agonist of nAChRs, caused catecholamine secretion corresponding to 18.90 ± 0.38 % of the total catecholamines in the cells. When the cells were treated with the same four flavonol glycosides at 10 μM for 10 min, ikarisoside A strongly reduced catecholamine secretion induced by ACh, to 6.83 ± 0.51 % of the total, whereas the other three had little effect (Fig. 2a). Veratridine (100 μM), an activator of voltage-dependent Na^+ channels, and 56 mM K^+, which depolarizes cell membranes and then activates voltage-dependent Ca^{2+} channels, also caused catecholamine secretion corresponding to 26.52 ± 0.88 % (Fig. 2b) and 20.51 ± 0.70 % (Fig. 2c) of the total catecholamines, respectively. Treatment of cells with these flavonol glycosides at 10 μM did not affect catecholamine secretion induced by veratridine (Fig. 2b) and 56 mM K^+ (Fig. 2c).

Concentration-inhibition curves for the effects of ikarisoside A on catecholamine secretion, $^{45}Ca^{2+}$ influx, and $^{22}Na^+$ influx induced by ACh

We examined the effects of ikarisoside A on catecholamine secretion, $^{45}Ca^{2+}$ influx, and $^{22}Na^+$ influx induced by ACh. Treatment of cells with ikarisoside A at 1, 3, 10, 30, and 100 μM significantly inhibited ACh-induced secretion of catecholamines (18.22 ± 0.16 % of the total catecholamines in the cells) to 15.36 ± 0.38 %, 12.27 ± 0.40 %, 7.68 ± 0.30 %, 5.33 ± 0.47 %, and 4.95 ± 0.25 % of the total catecholamines in the cells, respectively (Fig. 3a). Ikarisoside A also inhibited ACh-induced $^{45}Ca^{2+}$ influx and $^{22}Na^+$ influx in a concentration-dependent manner (Fig. 3b, c). The half-maximal inhibitory concentration (IC_{50}) of ikarisoside A in catecholamine secretion, $^{45}Ca^{2+}$ influx, and $^{22}Na^+$ influx are 4.00, 9.90, and 2.96 μM, respectively.

Inhibitory mode of ikarisoside A on ACh-induced catecholamine secretion in adrenal medullary cells

To investigate the mechanism by which ikarisoside A inhibits ACh-induced catecholamine secretion, we examined whether or not the inhibitory effect of ikarisoside A on catecholamine secretion is overcome when the ACh concentration is

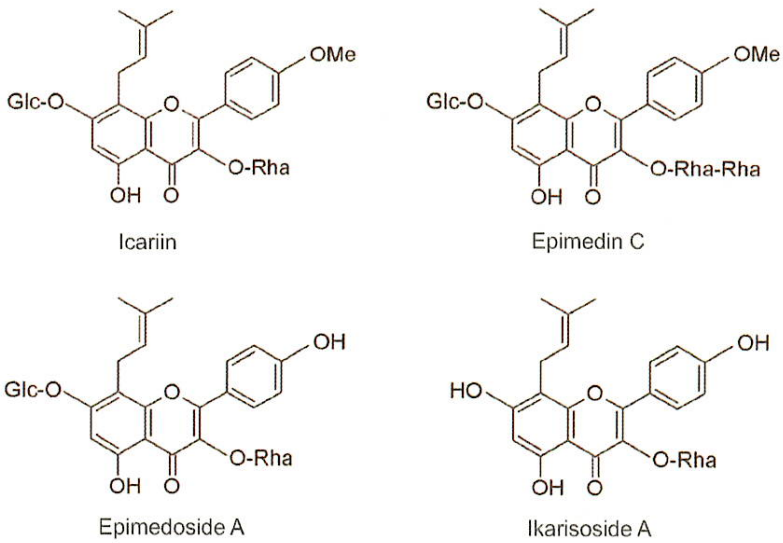

Fig. 1 Chemical structures of icariin, epimedin C, epimedoside A, ikarisoside A. The abbreviations Glc and Rha in the structures are glucose and rhamnose, respectively

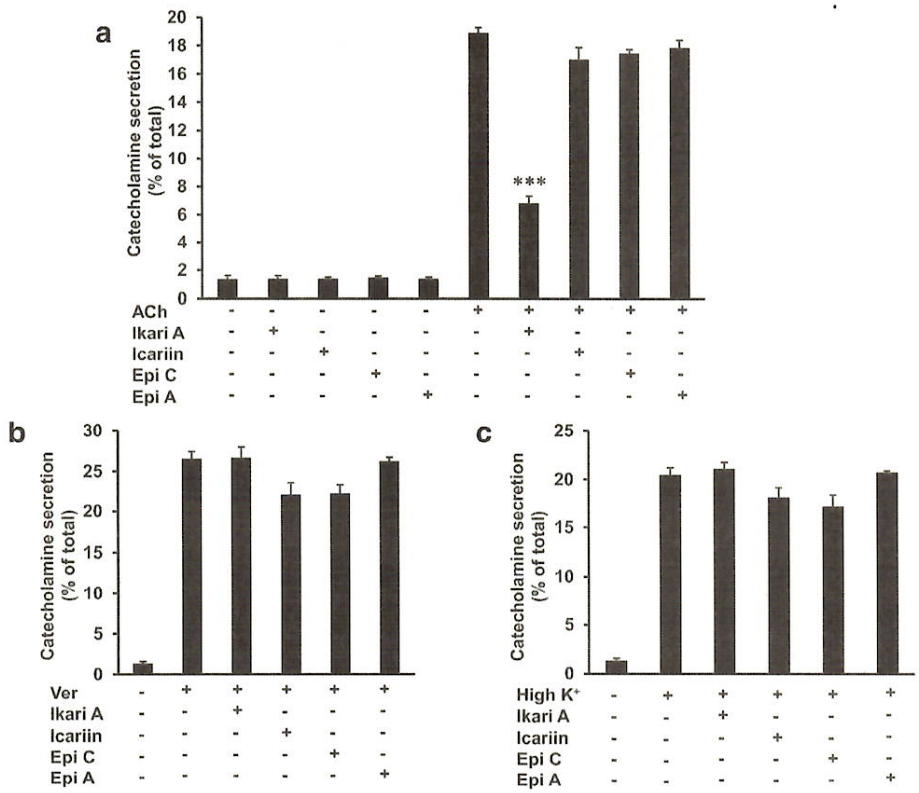

Fig. 2 Effects of ikarisoside A, icariin, epimedin C, or epimedoside A on catecholamine secretion induced by various secretagogues in cultured bovine adrenal medullary cells. After preincubation with cells with or without ikarisoside A (Ikari A) (10 μM), icariin (10 μM), epimedin C (Epi C) (10 μM), and epimedoside A (Epi A) (10 μM) for 10 min, the cells (10^6/well) were incubated with or without these four flavonol glycosides (10 μM), ACh (300 μM) (**a**), veratridine (100 μM) (**b**), or 56 mM K^+ (**c**) for another 10 min at 37 °C. Catecholamines secreted into the medium were expressed as a percentage of the total catecholamines in the cells. Data are means ± SEM from three separate experiments carried out in triplicate. ***$P < 0.001$, compared with ACh alone (analyzed by one-way ANOVA with Dunnett's multiple comparison post hoc test)

increased. Even when the ACh concentrations in the incubation medium increased from 3 to 300 μM, they did not overcome the inhibitory effect of ikarisoside A (Fig. 4a). Double-reciprocal plot analysis revealed that ikarisoside A exerts a noncompetitive type of inhibition on ACh-induced secretion of catecholamines (Fig. 4b).

Effects of ikarisoside A on ACh-induced inward current in *Xenopus* oocytes expressing α3β4 nAChRs

We examined the direct effects of ikarisoside A on ACh responses in *Xenopus* oocytes expressing rat α3β4 nAChRs. As shown in Fig. 5a, ikarisoside A reversibly inhibited ACh (0.2 mM)-induced currents. Ikarisoside A inhibited ACh-induced currents concentration dependently. It suppressed those currents to 80 ± 3 %, 69 ± 6 %, 43 ± 6 %, 32 ± 8 %, and 22 ± 5 % of the control at 0.1, 0.3, 1, 3, and 10 μM, respectively, and the inhibitory effects were significant from 0.10 μM onward; the IC_{50} was 0.48 μM (Fig. 5b).

Effect of aglycon of ikarisoside A on ACh-induced secretion of catecholamines

Ikarisoside A is a flavonol glycoside having one rhamnose at the 3 position in the chemical structure. 3,5,7-Trihydroxy-2-(4-hydroxyphenyl)-8-(3-methylbut-2-enyl)-4*H*-chromen-4-one is the aglycon of ikarisoside A. We examined the effect of this aglycon on ACh-induced secretion of catecholamines. As shown in Fig. 6, the aglycon of ikarisoside A did not affect basal or ACh-induced secretion of catecholamines.

Effect of ikarisoside A on ^{14}C-catecholamine synthesis from [^{14}C]tyrosine and tyrosine hydroxylase activity

As shown in Fig. 7a, ACh (300 μM) increased the synthesis of ^{14}C-catecholamines from [^{14}C]tyrosine about 3-fold in bovine adrenal medullary cells. The concurrent treatment of cells with ikarisoside A inhibited the stimulatory effect of 300 μM ACh on ^{14}C-catecholamine synthesis in a concentration (1–

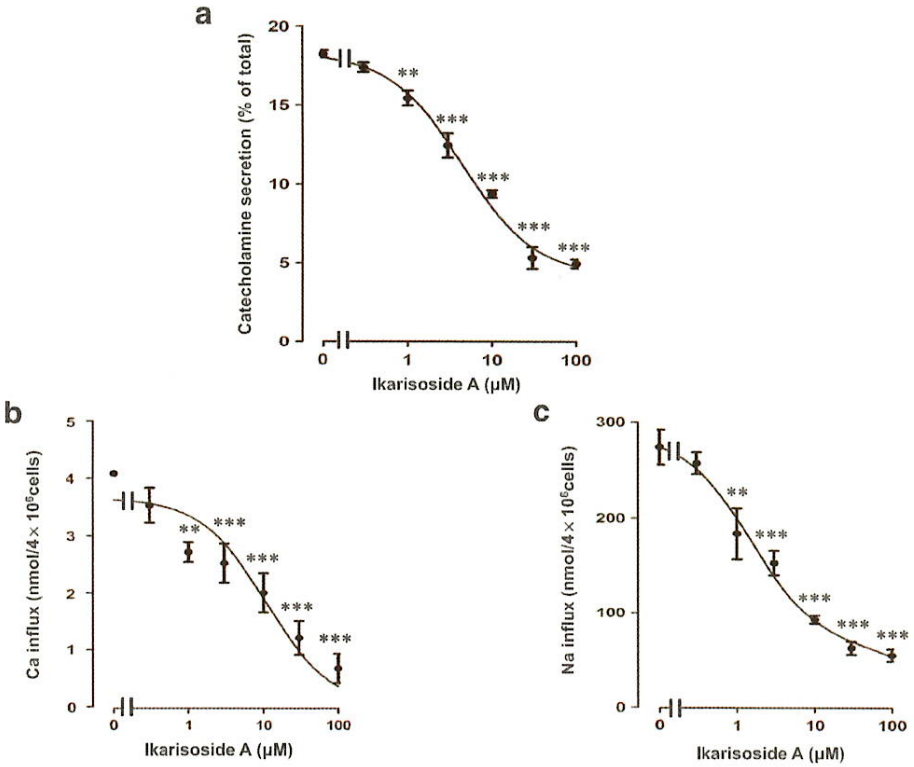

Fig. 3 Effects of ikarisoside A on catecholamine secretion (**a**), $^{45}Ca^{2+}$ influx (**b**), and $^{22}Na^{+}$ influx (**c**) induced by ACh. (**a**) After preincubation for 10 min with or without ikarisoside A (0.3–100 μM), cells were stimulated with ACh (300 μM) in the presence or absence of ikarisoside A (0.3–100 μM) for another 10 min at 37 °C. Catecholamines secreted into the medium were expressed as a percentage of the total catecholamines in the cells. **b**, **c** After preincubation for 10 min, cells were stimulated with ACh (300 μM) and 1.5 μCi of $^{45}CaCl_2$ (**b**) or $^{22}NaCl$ (**c**) in the presence or absence of ikarisoside A (0.3–100 μM) for another 5 min at 37 °C. $^{45}Ca^{2+}$ influx and $^{22}Na^{+}$ influx were measured and were expressed as nmol/4 × 10^6 cells. Data are means ± SEM from three separate experiments carried out in triplicate. $^{**}P < 0.01$ and $^{***}P < 0.001$, compared with ACh alone (analyzed by one-way ANOVA with Dunnett's multiple comparison post hoc test)

100 μM)-dependent manner (Fig. 7a), yielding an IC_{50} value of 2.85 μM. Ikarisoside A (1–100 μM) had little effect on the basal synthesis of ^{14}C-catecholamines.

We next examined the effect of ikarisoside A on tyrosine hydroxylase activity in the cells. After preincubation with or without ikarisoside A (0.1–100 μM) for 10 min, cells were incubated with 300 μM ACh in the absence or presence of ikarisoside A (0.1–100 μM) for another 10 min at 37 °C. Ikarisoside A (10–100 μM) inhibited the tyrosine hydroxylase activity induced by ACh and tended to inhibit the basal enzyme activity (Fig. 7b). The IC_{50} value of ikarisoside A for its inhibitory effect on the ACh-induced tyrosine hydroxylase activity was 9.13 μM (derived from the curve representing the difference between stimulated and basal tyrosine hydroxylase; not shown).

Discussion

In present study, we investigated the effects of four flavonol glycosides derived from the leaves of the genus *Epimedium*. We demonstrated that ikarisoside A, but not the other three, inhibited the secretion and synthesis of catecholamines induced by ACh in cultured bovine adrenal medullary cells. To our knowledge, this is the first direct evidence of an inhibitory effect of ikarisoside A on catecholamine secretion and synthesis in cultured bovine adrenal medullary cells.

Inhibitory effect of ikarisoside A on catecholamine secretion induced by ACh

The present study demonstrated that ikarisoside A significantly inhibits catecholamine secretion induced by ACh, but not by veratridine or 56 mM K^+ in adrenal medullary cells. We previously reported that ACh activates nAChR-ion channels, and induces Na^+ influx, subsequent Ca^{2+} influx, and finally catecholamine secretion. On the other hand, veratridine activates voltage-dependent Na^+ channels and 56 mM K^+ depolarizes cell membranes to activate voltage-dependent Ca^{2+} channels (Wada et al. 1984, 1985b). In the present study, ikarisoside A did not inhibit the stimulatory effects of veratridine and 56 mM K^+ on catecholamine secretion. Therefore,

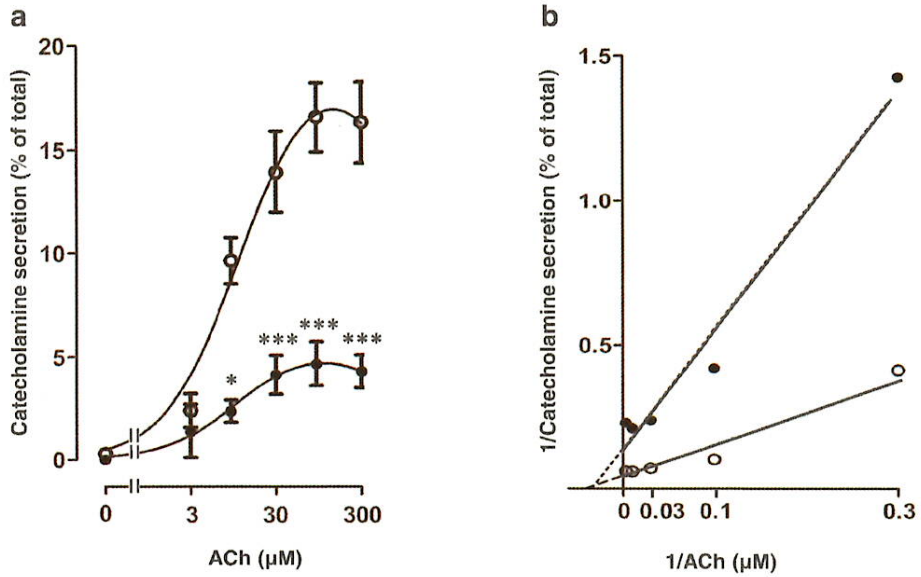

Fig. 4 Inhibitory mode of ikarisoside A on catecholamine secretion induced by ACh. **a** After preincubation for 10 min, cells were stimulated with (*black circle*) or without (*white circle*) ikarisoside A (10 μM) in the presence or absence of ACh (1–300 μM) for another 10 min at 37 °C. Catecholamines secreted into the medium were expressed as a percentage of the total catecholamines in the cells. Data are means + SEM from three separate experiments carried out in triplicate. The data of ACh plus ikarisoside A are shown by subtracting basal secretion obtained in the presence of ikarisoside A. $^{*}P < 0.05$ and $^{***}P < 0.001$, compared with ACh alone (analyzed by one-way ANOVA with Dunnett's multiple comparison post hoc test). **b** Double-reciprocal plot analysis of the data in (**a**)

ikarisoside A seems to inhibit nAChR-ion channels but not voltage-dependent Na^+ channels or voltage-dependent Ca^{2+} channels. Ikarisoside A inhibited Ca^{2+} influx and Na^+ influx induced by ACh in a concentration-dependent manner similar

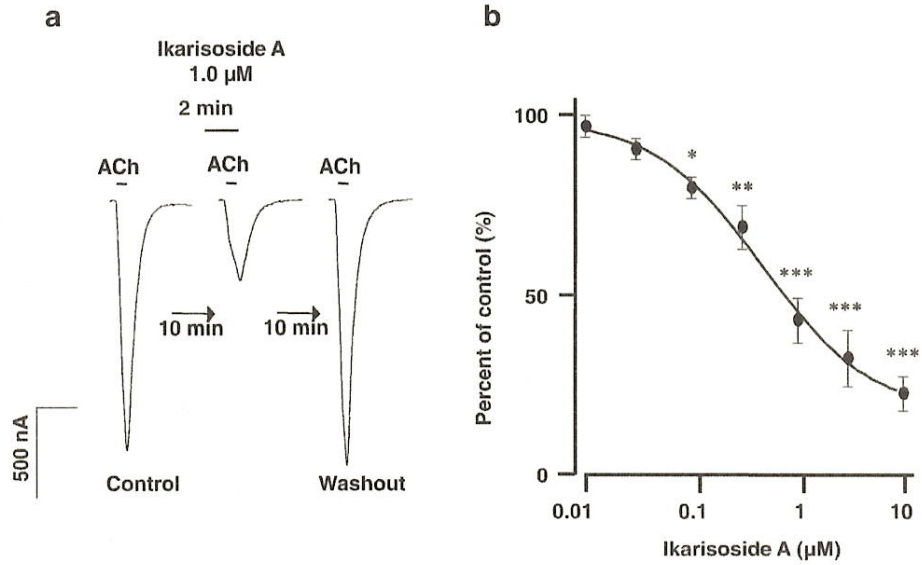

Fig. 5 Effects of ikarisoside A on peak ACh-induced inward currents in *Xenopus* oocytes expressing rat α3β4 nAChRs. **a** Representative traces from a single *Xenopus* oocyte are shown. The currents of ikarisoside A-treated oocytes were recorded 10 min after recording of the control currents, and the washout currents were obtained 10 min after ikarisoside A treatment. Ikarisoside A (1 μM) suppressed the currents induced by the EC_{50} (0.2 mM) of ACh, and the inhibitory effects were reversible. **b** Concentration-response curve for the inhibitory effects of ikarisoside A on ACh-induced currents. The peak current amplitude in the presence of ikarisoside A was normalized to that of the control and the effects are expressed as percentages of the control. Data are presented as means + SEM from four separate experiments carried out in triplicate. $^{*}P < 0.05$, $^{**}P < 0.01$, and $^{***}P < 0.001$, compared to the control (based on one-way ANOVA with Dunnett's multiple comparison post hoc test). Nonlinear regression analysis was performed and the mean value of IC_{50} for ikarisoside A is 0.48 μM

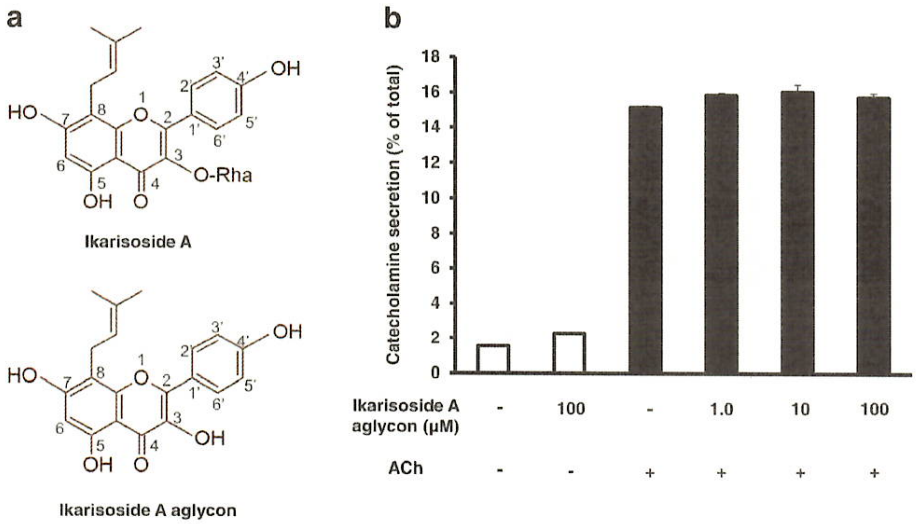

Fig. 6 Structure of ikarisoside A and its aglycon (**a**) and effect of aglycon of ikarisoside A on ACh-induced catecholamine secretion (**b**). **a** Structure of ikarisoside A and its aglycon (3,5,7-trihydroxy-2-(4-hydroxyphenyl)-8-(3-methylbut-2-enyl)-4*H*-chromen-4-one). **b** After preincubation with cells with or without aglycon of ikarisoside A (1–100 μM) for 10 min, the cells (10^6/well) were incubated with or without aglycon of ikarisoside A (1–100 μM) and ACh (300 μM) for another 10 min at 37 °C. Catecholamines secreted into the medium were expressed as a percentage of the total catecholamines in the cells. Data are means ± SEM from three separate experiments carried out in triplicate

to that of catecholamine secretion. In the exocytotic secretion of catecholamines, Ca^{2+} plays an indispensable role as the coupler in the stimulus-secretion coupling (Douglas and Rubin 1961, 1963). From these findings, it is likely that ikarisoside A inhibits ACh-induced catecholamine secretion by suppressing nAChR-ion channels. We investigated the inhibitory mode of ikarisoside A on nAChR-ion channels. Even when the concentration of ACh was increased, the inhibitory

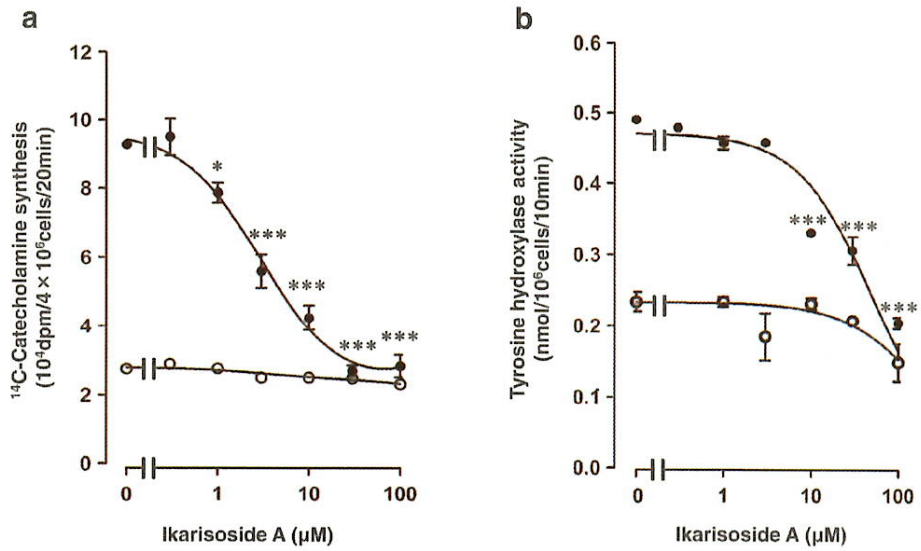

Fig. 7 Effects of ikarisoside A on ^{14}C-catecholamine synthesis from [^{14}C]tyrosine (**a**) and tyrosine hydroxylase activity (**b**) in the cells. **a** After preincubation for 10 min with or without ikarisoside A (0.1–100 μM), cells (4 × 10^6/dish) were incubated with L-[U-^{14}C] tyrosine (20 μM, 1 μCi) in the presence or absence of ikarisoside A (0.1–100 μM) and with (*black circle*) or without (*white circle*) 300 μM ACh at 37 °C for 20 min. The ^{14}C-catecholamines formed were measured. **b** After preincubation with or without ikarisoside A (0.1–100 μM) for 10 min, cells (10^6/well) were incubated with L-[1-^{14}C] tyrosine (18 μM, 0.2 μCi) in the presence or absence of ikarisoside A (0.1–100 μM) and with (*black circle*) or without (*white circle*) 300 μM ACh at 37 °C for 10 min, and tyrosine hydroxylase activity was measured. Data are means + SEM from three separate experiments carried out in triplicate. $^*P < 0.05$ and $^{***}P < 0.001$, compared with ACh alone (analyzed by one-way ANOVA with Dunnett's multiple comparison post hoc test)

effect of ikarisoside A on ACh-induced secretion of catecholamines was not overcome, suggesting a noncompetitive inhibition and that ikarisoside A acts at a site different from that for ACh binding. A previous review (Lena and Changeux 1993) reported that the site at which noncompetitive blockers act lies at the interface between the nicotinic receptor protein and the membrane lipids.

In the *Xenopus* oocytes expressed with α3β4 nAChRs, ikarisoside A directly inhibited ACh-induced current. The IC_{50} values of ikarisoside A for $^{22}Na^+$ influx in adrenal medullary cells and for Na^+ current in the oocytes were 2.96 and 0.48 μM, respectively. The IC_{50} in the bovine adrenal medullary cells is 6.2-fold bigger than that of the drug in the oocyte system. Although the reason for the discrepancy of the IC_{50} between the two systems is not yet clear, the discrepancy may be explained in the following way. (1) A maximally effective concentration of ACh was used for the $^{22}Na^+$ influx experiments in bovine adrenal medullary cells but the half-maximal concentration was used for the Na^+ current in the oocyte system. (2) In the oocyte expression system, there may be some changes in the test compound potency compared to that of the method using mammalian cells, i.e., a decrease (Lambert et al. 2001; Akk et al. 2008) or an increase (Pintado et al. 2000) in the sensitivity of test compounds. (3) Bovine adrenal medullary cells express multiple nAChR subtypes such as α3β4 (Criado et al. 1992; Garcia-Guzman et al. 1995), α3β4α5 (Campos-Caro et al. 1997), and α7 (Lopez et al. 1998). We should study above possibilities and examine the effect of ikarisoside A on the function of nAChRs in other mammalian cells.

Structure-activity relationship of ikarisoside A for inhibition of nAChR-ion channels

In the present study, we used four flavonol glycosides derived from the *Epimedium* species. Ikarisoside A, but not the other three flavonols, inhibited the functioning of nAChR-ion channels. Judging from the differences in their structures, ikarisoside A has a hydroxyl group at the 7 position in the structure whereas other three have a glucose moiety at this position, suggesting that a glucose moiety at the 7 position may induce stereo-specific interference when flavonol glycosides interact with nAChRs. Furthermore, the inhibition of ACh-induced secretion by ikarisoside A disappeared by the removal of the rhamnose moiety at the 3 position from ikarisoside A. These findings suggest that the rhamnose moiety at the 3 position of ikarisoside A is essential to inhibit the function of nAChR-ion channels.

Inhibitory effect of ikarisoside A on catecholamine synthesis

Ikarisoside A inhibited not only catecholamine secretion but also reduced catecholamine synthesis in ACh-stimulated cells. In the regulation of catecholamine synthesis, Ca^{2+} plays an important role as the coupler in the stimulus-synthesis coupling (Yanagihara et al. 1987) as well as in the stimulus-secretion coupling (Douglas and Rubin 1961, 1963). In the present study, we observed that ikarisoside A suppressed the $^{22}Na^+$ influx and the subsequent $^{45}Ca^{2+}$ influx by inhibiting nAChR-ion channels. Therefore, it is likely that ikarisoside A inhibits catecholamine synthesis and tyrosine hydroxylase activity induced by ACh via the suppression of Ca^{2+} influx in cultured bovine adrenal medulla cells. In harmony with this view, the IC_{50} values of ikarisoside A for inhibition of $^{22}Na^+$ and $^{45}Ca^{2+}$ influx and for inhibition of catecholamine synthesis and tyrosine hydroxylase are very similar.

Pharmacological significance of the inhibitory effects of ikarisoside A on adrenal medullary functions

The human serum concentration of ikarisoside A has not been reported yet. Several previous in vitro studies reported that ikarisoside A at 5.0–20 μM inhibits osteoclastogenic differentiation and nitric oxide synthase in murine monocyte/macrophage cell line RAW264.7 cells (Choi et al. 2008, 2010) and induces neurite outgrowth activity in PC12h cells at 10 μM (Kuroda et al. 2000). In the present study, we observed a significant inhibition of ikarisoside A at 0.1 and 1.0 μM in ACh-induced current in *Xenopus* oocytes and ACh-induced synthesis and secretion of catecholamines, respectively.

It is well known that adrenaline and noradrenaline have an important role in the regulation of normal function in the central and peripheral sympathetic nervous systems. Under strong and prolonged stress, an increased catecholamine release may occur, which possibly induces cardiovascular diseases such as hypertension, atherosclerosis, coronary heart disease, and heart failure (Yanagihara et al. 2014). Chronic heart failure is reported to be associated with the activation of the sympathetic nervous system as manifested by increased circulating catecholamines (Westfall and Westfall 2011). Furthermore, Hara et al. (2011) reported that the stress hormone adrenaline stimulates β_2-adrenoceptors, which activates the Gs protein/cyclic AMP-dependent protein kinase and the β-arrestin-mediated signaling pathway, reduces the p53 level, and induces DNA damage.

Our previous studies reported that daidzein, a soy isoflavone, (Liu et al. 2007) and nobiletin, a citrus polymethoxy flavone, (Zhang et al. 2010) suppress the secretion and synthesis of catecholamines induced by ACh in cultured bovine adrenal medullary cells. In addition to these flavonoids, ikarisoside A also may protect the hyperactive catecholamine system induced by strong stress or emotional excitation which evokes the secretion of ACh from the splanchnic nerves. Further in vivo experiments will provide more conclusive information on ikarisoside A and promote the development of a

therapeutic drug for stress-induced disorders associated with mental or cardiovascular diseases.

Acknowledgments This work was supported, in part, by Grant-in-Aid (23617035, 23617036, 23590159, and 26350170) for Scientific Research (C) from the Japan Society for the Promotion of Science.

Conflict of interest The authors declare that they have no competing interests.

References

Akk G, Li P, Bracamontes J, Reichert DE, Covey DF, Steinbach JH (2008) Mutations of the $GABA_A$ receptor α1 subunit M1 domain reveal unexpected complexity for modulation by neuroactive steroids. Mol Pharmacol 74:614–627

Bobrovskaya L, Cheah TB, Bunn SJ, Dunkley PR (1998) Tyrosine hydroxylase in bovine adrenal chromaffin cells: angiotensin II-stimulated activity and phosphorylation of Ser^{19}, Ser^{31}, and Ser^{40}. J Neurochem 70:2565–2573

Campos-Caro A, Smillie FI, Dominguez del Toro E, Rovira JC, Vicente-Agullo F, Chapuli J, Juiz JM, Sala S, Sala F, Ballesta JJ, Criado M (1997) Neuronal nicotinic acetylcholine receptors on bovine chromaffin cells: cloning, expression, and genomic organization of receptor subunits. J Neurochem 68:488–497

Chen WF, Mok SK, Wang XL, Lai KH, Lai WP, Luk HK, Leung PC, Yao XS, Wong MS (2011) Total flavonoid fraction of the herba epimedii extract suppresses urinary calcium excretion and improves bone properties in ovariectomised mice. Br J Nutr 105:180–189

Choi HJ, Eun JS, Park YR, Kim DK, Li R, Moon WS, Park JM, Kim HS, Cho NP, Cho SD, Soh Y (2008) Ikarisoside A inhibits inducible nitric oxide synthase in lipopolysaccharide-stimulated RAW 264.7 cells via p38 kinase and nuclear factor-κB signaling pathways. Eur J Pharmacol 601:171–178

Choi HJ, Park YR, Nepal M, Choi BY, Cho NP, Choi SH, Heo SR, Kim HS, Yang MS, Soh Y (2010) Inhibition of osteoclastogenic differentiation by Ikarisoside A in RAW 264.7 cells via JNK and NF-κB signaling pathways. Eur J Pharmacol 636:28–35

Criado M, Alamo L, Navarro A (1992) Primary structure of an agonist binding subunit of the nicotinic acetylcholine receptor from bovine adrenal chromaffin cells. Neurochem Res 17:281–287

Dou J, Liu Z, Liu S (2006) Structure identification of a prenylflavonol glycoside from epimedium koreanum by electrospray ionization tandem mass spectrometry. Anal Sci 22:449–452

Douglas WW, Rubin RP (1961) Mechanism of nicotinic action at the adrenal medulla: calcium as a link in stimulus-secretion coupling. Nature 192:1087–1089

Douglas WW, Rubin RP (1963) The mechanism of catecholamine release from the adrenal medulla and the role of calcium in stimulus-secretion coupling. J Physiol 167:288–310

Garcia-Guzman M, Sala F, Sala S, Campos-Caro A, Stuhmer W, Gutierrez LM, Criado M (1995) α-Bungarotoxin-sensitive nicotinic receptors on bovine chromaffin cells: molecular cloning, functional expression and alternative splicing of the α7 subunit. Eur J Neurosci 7:647–655

Hara MR, Kovacs JJ, Whalen EJ, Rajagopal S, Strachan RT, Grant W, Towers AJ, Williams B, Lam CM, Xiao K, Shenoy SK, Gregory SG, Ahn S, Duckett DR, Lefkowitz RJ (2011) A stress response pathway regulates DNA damage through β_2-adrenoreceptors and β-arrestin-1. Nature 477:349–353

Horishita T, Harris RA (2008) n-Alcohols inhibit voltage-gated Na^+ channels expressed in Xenopus oocytes. J Pharmacol Exp Ther 326:270–277

Kajiwara K, Yanagita T, Nakashima Y, Wada A, Izumi F, Yanagihara N (2002) Differential effects of short and prolonged exposure to carvedilol on voltage-dependent Na^+ channels in cultured bovine adrenal medullary cells. J Pharmacol Exp Ther 302:212–218

Kuroda M, Mimaki Y, Sashida Y, Umegaki E, Yamazaki M, Chiba K, Mohri T, Kitahara M, Yasuda A, Naoi N, Xu ZW, Li MR (2000) Flavonol glycosides from Epimedium sagittatum and their neurite outgrowth activity on PC12h cells. Planta Med 66:575–577

Lai X, Ye Y, Sun C, Huang X, Tang X, Zeng X, Yin P, Zeng Y (2013) Icaritin exhibits anti-inflammatory effects in the mouse peritoneal macrophages and peritonitis model. Int Immunopharmacol 16:41–49

Lambert JJ, Belelli D, Harney SC, Peters JA, Frenguelli BG (2001) Modulation of native and recombinant $GABA_A$ receptors by endogenous and synthetic neuroactive steroids. Brain Res Brain Res Rev 37:68–80

Lena C, Changeux JP (1993) Allosteric modulations of the nicotinic acetylcholine receptor. Trends Neurosci 16:181–186

Liu M, Yanagihara N, Toyohira Y, Tsutsui M, Ueno S, Shinohara Y (2007) Dual effects of daidzein, a soy isoflavone, on catecholamine synthesis and secretion in cultured bovine adrenal medullary cells. Endocrinology 148:5348–5354

Lopez MG, Montiel C, Herrero CJ, Garcia-Palomero E, Mayorgas I, Hernandez-Guijo JM, Villarroya M, Olivares R, Gandia L, McIntosh JM, Olivera BM, Garcia AG (1998) Unmasking the functions of the chromaffin cell α7 nicotinic receptor by using short pulses of acetylcholine and selective blockers. Proc Natl Acad Sci U S A 95:14184–14189

Lu MF, Xiao ZT, Zhang HY (2013) Where do health benefits of flavonoids come from? Insights from flavonoid targets and their evolutionary history. Biochem Biophys Res Commun 434:701–704

Mizuno M, Iinuma M, Tanaka T, Sakakibara N, Hanioka S (1988) Flavonol glycosides in Epimedium species. Chem Pharm Bull 36(9):3487–3490

Nagatsu T, Levitt M, Udenfriend S (1964) Tyrosine hydroxylase. The initial step in norepinephrine biosynthesis. J Biol Chem 239:2910–2917

Nijveldt RJ, van Nood E, van Hoorn DE, Boelens PG, van Norren K, van Leeuwen PA (2001) Flavonoids: a review of probable mechanisms of action and potential applications. Am J Clin Nutr 74:418–425

Pintado AJ, Herrero CJ, Garcia AG, Montiel C (2000) The novel Na^+/Ca^{2+} exchange inhibitor KB-R7943 also blocks native and expressed neuronal nicotinic receptors. Br J Pharmacol 130:1893–1902

Ren ZL, Zuo PP (2012) Neural regeneration: role of traditional Chinese medicine in neurological diseases treatment. J Pharmacol Sci 120:139–145

Shinohara Y, Toyohira Y, Ueno S, Liu M, Tsutsui M, Yanagihara N (2007) Effects of resveratrol, a grape polyphenol, on catecholamine secretion and synthesis in cultured bovine adrenal medullary cells. Biochem Pharmacol 74:1608–1618

Toyohira Y, Kubo T, Watanabe M, Uezono Y, Ueno S, Shinkai K, Tsutsui M, Izumi F, Yanagihara N (2005) Selective blockade of nicotinic acetylcholine receptors by pimobendan, a drug for the treatment of heart failure: reduction of catecholamine secretion and synthesis in adrenal medullary cells. Naunyn Schmiedeberg's Arch Pharmacol 371:107–113

Tsutsui M, Yanagihara N, Miyamoto E, Kuroiwa A, Izumi F (1994) Correlation of activation of Ca^{2+}/calmodulin-dependent protein kinase II with catecholamine secretion and tyrosine hydroxylase activation in cultured bovine adrenal medullary cells. Mol Pharmacol 46:1041–1047

Ueno S, Tsutsui M, Toyohira Y, Minami K, Yanagihara N (2004) Sites of positive allosteric modulation by neurosteroids on ionotropic γ-aminobutyric acid receptor subunits. FEBS Lett 566:213–217

Wada A, Izumi F, Yanagihara N, Kobayashi H (1985a) Modulation by ouabain and diphenylhydantoin of veratridine-induced ^{22}Na influx and its relation to ^{45}Ca influx and the secretion of catecholamines in cultured bovine adrenal medullary cells. Naunyn Schmiedeberg's Arch Pharmacol 328:273–278

Wada A, Takara H, Izumi F, Kobayashi H, Yanagihara N (1985b) Influx of ^{22}Na through acetylcholine receptor-associated Na channels: relationship between ^{22}Na influx, ^{45}Ca influx and secretion of catecholamines in cultured bovine adrenal medulla cells. Neuroscience 15:283–292

Wada A, Yashima N, Izumi F, Kobayashi H, Yanagihara N (1984) Involvement of Na influx in acetylcholine receptor mediated secretion of catecholamines from cultured bovine adrenal medulla cells. Neurosci Lett 47:75–80

Weil-Malherbe H, Bone AD (1952) The chemical estimation of adrenaline-like substances in blood. Biochem J 51:311–318

Westfall TC and Westfall DP (2011) Adrenergic agonists and antagonists, in Goodman & Gilman's the pharmacological basis of therapeutics, 12th edn (Brunton LL, Chabner BC, and Knollmann BC, eds), pp. 277-330. McGraw-Hill, NY

Yanagihara N, Isosaki M, Ohuchi T, Oka M (1979) Muscarinic receptor-mediated increase in cyclic GMP level in isolated bovine adrenal medullary cells. FEBS Lett 105:296–298

Yanagihara N, Oishi Y, Yamamoto H, Tsutsui M, Kondoh J, Sugiura T, Miyamoto E, Izumi F (1996) Phosphorylation of chromogranin A and catecholamine secretion stimulated by elevation of intracellular Ca^{2+} in cultured bovine adrenal medullary cells. J Biol Chem 271: 17463–17468

Yanagihara N, Wada A, Izumi F (1987) Effects of α_2-adrenergic agonists on carbachol-stimulated catecholamine synthesis in cultured bovine adrenal medullary cells. Biochem Pharmacol 36:3823–3828

Yanagihara N, Zhang H, Toyohira Y, Takahashi K, Ueno S, Tsutsui M (2014) New insights into the pharmacological potential of plant flavonoids in the catecholamine system. J Pharmacol Sci 124:123–128

Zhang H, Toyohira Y, Ueno S, Shinohara Y, Itoh H, Furuno Y, Yamakuni T, Tsutsui M, Takahashi K, Yanagihara N (2010) Dual effects of nobiletin, a citrus polymethoxy flavone, on catecholamine secretion in cultured bovine adrenal medullary cells. J Neurochem 114:1030–1038

Zhou J, Chen KM, Ge BF, Ma XN, Guo XY, Cheng K, Gao YH, Yan LJ, Shi WG (2013) Comparison between icariin and genistein in osteogenic activity of marrow stromal cells. Zhongguo Zhong Yao Za Zhi 38:1783–1788